HIGH-DENSITY SHALLOW SHEAR WAVE VELOCITY CHARACTERISATION OF THE URBAN CHRISTCHURCH, NEW ZEALAND REGION

Christopher R. McGann
Brendon A. Bradley
Misko Cubrinovski

Research Report 2015-02

Department of Civil and Natural Resources Engineering
University of Canterbury
Christchurch, New Zealand

April 16, 2015

Acknowledgements

Funding for this work was provided by the New Zealand Earthquake Commission (EQC) and the Natural Hazards Research Platform (NHRP). The authors would also like to thank the Canterbury Geotechnical Database team for providing access to the data used in this study, and Matthew Hughes for assistance with the graphics in Fig. 2.4.

Executive Summary

This report summarizes the development of a region-wide surficial soil shear wave velocity (V_s) model based on the unique combination of a large high-spatial-density database of cone penetration test (CPT) logs in the greater Christchurch urban area ($> 15,000$ logs as of 1 February 2014) and the Christchurch-specific empirical correlation between soil V_s and CPT data developed by McGann et al. [1, 2]. This model has applications for site characterization efforts via maps of time-averaged V_s over specific depths (e.g. Vs30, Vs10), and for numerical modeling efforts via the identification of typical V_s profiles for different regions and soil behaviour types within Christchurch. In addition, the V_s model can be used to constrain the near-surface velocities for the 3D seismic velocity model of the Canterbury basin [3] currently being developed for the purpose of broadband ground motion simulation. The general development of these region-wide near-surface V_s models includes the following general phases, with each discussed in separate chapters of this report.

- An evaluation of the available CPT dataset for suitability, and the definition of other datasets and assumptions necessary to characterize the surficial sediments of the region to 30 m depth.

- The development of time-averaged shear wave velocity (V_{sz}) surfaces for the Christchurch area from the adopted CPT dataset (and supplementary data/assumptions) using spatial interpolation. The V_{sz} surfaces are used to explore the characteristics of the near-surface soils in the regions and are shown to correspond well with known features of the local geology, the historical ecosystems of the area, and observations made following the 2010-2011 Canterbury earthquakes.

- A detailed analysis of the V_s profiles in eight subregions of Christchurch is performed to assess the variablity in the soil profiles for regions with similar V_{sz} values and to assess V_{sz} as a predictive metric for local site response.

It is shown that the distrubution of soil shear wave velocity in the Christchurch regions is highly variable both spatially (horizontally) and with depth (vertically) due to the varied geological histories for different parts of the area, and the highly stratified nature of the near-surface deposits. This variability is not considered to be greatly significant in terms of current simplified site classification systems; based on computed V_{s30} values, all considered regions can be categorized as NEHRP sites class D ($180 < V_s < 360$ m/s) or E ($V_s < 180$ m/s), however, detailed analysis of the shear wave velocity profiles in different subregions of Christchurch show that the expected surficial site response can vary quite a bit across the region despite the relative similarity in V_{s30}.

Table of Contents

Chapter 1

Introduction

The 2010-2011 Canterbury earthquake sequence [4–9] resulted in widespread damage, and continuing disruption, to the infrastructure of Christchurch at a level unprecedented in New Zealand history. The 4 September 2010 M_w7.1 Darfield earthquake was the first event in the sequence, occurring 15 km west of central Christchurch city, and resulting in moderate damage to local infrastructure and widespread liquefaction [10]. The 22 February 2011 M_w6.2 Christchurch earthquake occurred approximately 4 km southwest of the city center, and the high-frequency amplitudes of the resulting ground motions experienced across most of the city were much larger than in the Darfield event [4, 5]. The 22 February 2011 earthquake resulted in significant damage to infrastructure, with significant structural damage observed in a large number of commercial buildings in the central business district (CBD). Liquefaction and lateral spreading associated with the Christchurch earthquake were significantly more severe and widespread than was observed the previous September, and accounted for the majority of the severe damage to properties.

The significant spatial variability of surficial ground motions recorded from these two strong earthquakes illustrates the importance of local site effects (seismic response of surficial soils) on surface ground motion and the importance of site-specific response analysis. The response spectra for both events were similar at multiple strong motion stations despite the clear differences in source and path effects [6], though this was not the case at stations underlain by liquefiable soils. For the stations with dissimilar responses for the two strong events, in addition to the differences due to source and path effects, the differences in the two events led to different site responses. The increased amplitudes characteristic of the Christchurch earthquake resulted in larger shear deformation and associated excess pore pressure build-up compared to the Darfield event, and thus, the occurrence of liquefaction-related phenomena was more significant and widespread. Several strong motion stations were located in areas where liquefaction was prevalent during the February event, but was not observed following the September earthquake, and the resulting differences in the recorded ground motions at these stations provide evidence for the importance of site-specific analysis [6].

Design and building codes in New Zealand, and internationally, typically provide a site classification system with which to group soil deposits with continuously-varying, and often highly variable, strength and stiffness properties into a series of discrete categories. Such site classification systems inherently assume that it is acceptable for design purposes to account for local site effects in an approximate manner in lieu of site-specific characterization, and each site class provides distinct seismic design considerations based on the general expected soil response represented by the chosen classification system to be used as guidance in the design of structures. Site classification systems are typically based on a simplified metric, or set of metrics, intended to describe soil conditions in a general manner. Travel time-averaged shear wave velocity to 30 m depth (V_{s30}) is the primary site classification metric currently used internationally; in the United States via the National Earthquake Hazards Reduction Program (NEHRP) [11, 12] site classes, and in Europe via Eurocode 8 [13]. In New Zealand, the seismic design specifications contained in NZS1170.5:2004 [14] prescribe site classification based primarily on the low-amplitude site period, taken as four times the estimated or measured travel time of shear waves from the surface to underlying rock, with the soil-to-rock transition defined by a compressive strength of at least

1 MPa. Ground motion prediction equations (GMPEs) also use V_{s30} as an explanatory metric for site effects, both in New Zealand [15, 16] and internationally [e.g., 17]. Due to the ubiquity of V_{s30} as a distinguishing variable for site classification purposes, and due to the general utility of shear wave velocity (V_s) as a descriptor of soil conditions, a detailed characterization of the near-surface (depth < 30 m) V_s profile for the Christchurch region is a valuable tool for use in identifying and learning from the processes resulting in the strong ground motions observed in the 2010-2011 earthquakes.

The greater Christchurch urban area is located on the east coast of the south island of New Zealand, in the broad and relatively flat Canterbury plains that extend east from the Southern Alps to the Pacific coastline. Christchurch is bounded on the east by Pegasus Bay, on the south by the Port Hills, which are the northern rim of the extinct Lyttelton Volcano [18], and is surrounded by primarily rural lands to the north and west. The Canterbury plains are predominantly composed of alluvial sands and gravels deposited by rivers flowing from the Alps, though the coastal margins that underly the eastern suburbs of Christchurch are primarily composed of marine and active dune sands. Two spring-fed river systems flow through Christchurch, the Avon and Heathcote rivers, and the larger Waimakariri and Ashley rivers, which flow out of the Southern Alps, are located to the north of the primary Christchurch urban area. The Avon and Heathcote rivers terminate in the shared Avon-Heathcote Estuary located to the south east of the Christchurch central business district (CBD). The Holocene-age alluvial and coastal sediments that comprise the majority of the near-surface soils in the Christchurch area are directly underlain by the Riccarton Gravel, which is the uppermost gravel layer in an interbedded series of gravels and marine sediments alternately laid down during glacial and post-glacial periods. The Riccarton Gravel ranges in depth below the ground surface from about 15 m in the western suburbs to about 40 m in the east, and the depth of the Riccarton Gravel at a particular site is an important feature in the soil profile due to the velocity contrast that exists between the dense gravel and the looser surficial sediments.

Much of the damage incurred to residential and commercial structures in Christchurch by the 2010-2011 Canterbury earthquakes was geotechnical in nature (e.g. the widespread and severe liquefaction and lateral spreading that occurred throughout the area [10, 19, 20]). As a result, the post-earthquake recovery efforts in Christchurch have involved a significant focus on the characterization of the near-surface soil conditions in the region through subsurface explorations. Thousands of individual site exploration records obtained through borehole/standard penetration tests (SPT), cone penetration tests (CPT), surface wave analysis methods, and other testing approaches have been made available for use in research efforts through the Canterbury Geotechnical Database [21] project sponsored by the New Zealand Earthquake Commission (EQC) and the Canterbury Earthquake Recovery Authority (CERA). In this study, the available CPT data (> 15000 individual records as of 1 February 2014) is used in conjunction with the Christchurch-specific CPT-V_s correlation of McGann et al. [1, 2] to develop the desired characterization of the near-surface shear wave velocities in the region. This empirical CPT-V_s relationship was developed from seismic cone penetration test (SCPT) data from 86 alluvial and marine soil sites located throughout the greater Christchurch area using multiple linear regression with consideration for non-constant depth variance to account for the greater uncertainties observed at shallow depths. The CPT-V_s model was shown to perform well in forward predictions using synthetic profiles representative of a variety of soil types in McGann et al. [2], and was compared favorably to V_s profiles independently-obtained using surface-wave analysis techniques at several Christchurch strong motion stations (SMS) in McGann et al. [22].

This report presents the development of a shallow shear wave velocity model of the greater Christchurch urban area. The Christchurch-specific CPT-V_s model is applied to the large, high-spatial-density dataset of CPT records made available through the Canterbury Geotechnical

Database [21] to obtain the necessary characterization of the shear wave velocity in the CPT-penetrable near-surface (depth $z < 30$ m) alluvial, estuarine, marine/dune, and wetland deposits that are spread across the area. Due to the presence of the Riccarton Gravel in the upper 30 m zone beneath the majority of the region, an estimated surface for the depth to the top of the Riccarton Gravel developed using well log data is used to supplement the CPT-based V_s profiles where appropriate. To characterize the spatial and depth variability of V_s in the considered region, travel time-averaged shear wave velocities, V_{sz}, are calculated for target profile depths $z = 5$, 10, 20, and 30 m. Detailed analysis of specific subregions of Christchurch is also undertaken to examine the differences in V_s with depth for regions with similar V_{sz} values, and comparisons of the transfer functions obtained from typical V_s profiles for the considered subregions are made to assess the effects of the observed differences on the expected low-amplitude seismic site response.

Chapter 2

Datasets and Assumptions

2.1 CPT Dataset Summary

The CPT data referenced in this report includes 13670 individual CPT records extracted from the Canterbury Geotechnical Database [21] on 1 February 2014 from sites located throughout Christchurch and the surrounding towns and suburbs. This CPT data was primarily obtained to aid in the assessment of insurance claims[1]made after the events of the 2010-2011 Canterbury earthquake sequence and to help establish the residential land zoning categories used by the Canterbury Earthquake Recovery Authority (CERA) [23] to assess the viability of rebuilding in liquefaction-affected areas. Though these CPT records were not originally acquired with the intention of a subsequent region-wide near-surface soil characterization, they represent an unparallelled resource in terms of scope and spatial density of subsurface data, and present a unique opportunity for understanding the nature of the soils in the greater Christchurch area.

The CPT data obtained for the Canterbury Geotechnical Database sites are representative of a variety of soil types and site conditions typical to the region. These records generally cover the range of depths extending from the ground surface to the upper surface of the Riccarton Gravel that exists beneath Christchurch, though a large portion of the CPT tests were terminated at a pre-defined target depth (typically 20 m) or upon effective refusal due to a cobble, boulder, or dense gravel layer (Springston Formation) encountered above the Riccarton Gravel. As discussed in the following sections, the raw CPT measurement data from the adopted dataset was evaluated for suitability using a series of filters and exclusion criteria to ensure that only sites with consistent and useful data are used in the subsequent analysis and development steps.

2.1.1 CPT Data Processing Criteria

The data processing procedure developed to evaluate the raw CPT records for suitability of use is summarized in Fig. 2.1. This chart shows the order in which the various steps were carried out and indicates the number of CPT records (if any) removed from the dataset in each processing step. The initial criteria were established for the zone of soil immediately below the ground surface (pre-drill zone), as this region is often poorly characterized by the CPT due to lack of confinement, and many of the CPT sites made use of an approximately 0.5-1.5 m pre-drilled or hand-dug-and-backfilled hole as a starting point for the test to ensure infrastructure clearance. In order to consider this pre-drill zone consistently for the entire database, the end of the pre-drill zone, z_p, was defined as the first depth where the corrected dimensionless tip resistance [24, 25], $q_{c1N} > 50$ and $V_s > 65$ m/s. At any site where this depth was < 1 m, z_p was set equal to 1 m. A number of records did not meet this criteria at any depth were removed from the dataset. The values of q_c and f_s for $z \leq z_p$ were taken as constants, and set equal to the values at z_p. Any sites where the length of the pre-drill zone was more than 30% of the total profile length were fully excluded from the processed CPT dataset.

---

[1]**Note:** The Canterbury Geotechnical Database was prepared and/or compiled for the Earthquake Commission (EQC) to assist in assessing insurance claims made under the Earthquake Commission Act 1993 and/or for the Canterbury Earthquake Recovery Authority (CERA). The source maps and data were not intended for any other purpose. EQC, CERA, their data suppliers and their engineers, Tonkin & Taylor, have no liability for any use of the maps and data or for the consequences of any person relying on them in any way.

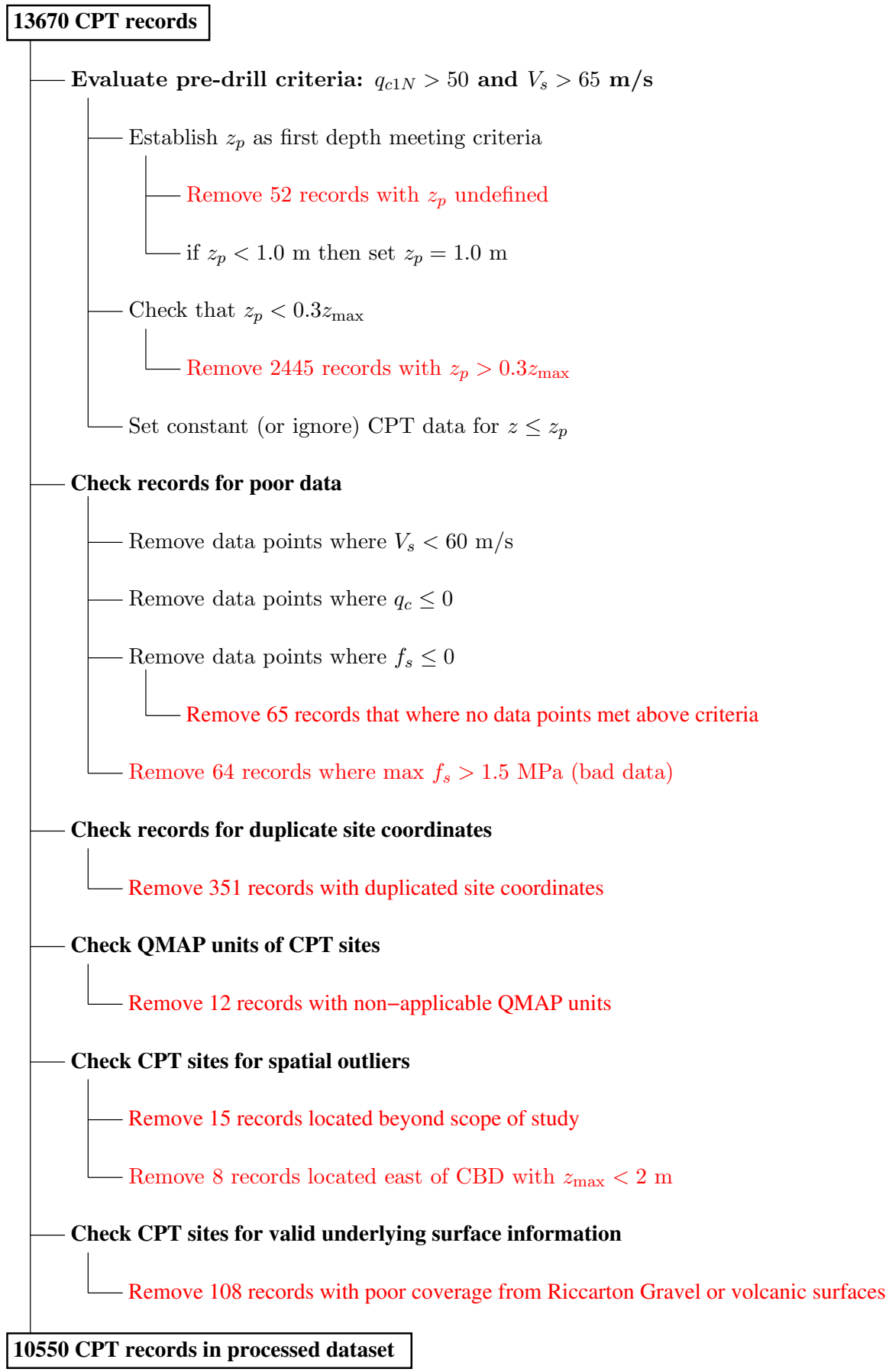

Fig. 2.1: Summary of data processing steps indicating order of operations and number of records removed in each step.

Beyond the pre-drill criteria, the quality of the data in each CPT record was evaluated. All readings with $q_c \leq 0$ MPa, $f_s \leq 0$ MPa, or $V_s < 60$ m/s were removed from the CPT profiles, and records with excessively large friction readings ($f_s > 1.5$ MPa anywhere in profile) were excluded from the processed dataset due to the questionable validity of these readings. A number of CPT sites were listed with identical locations to one or more other CPT sites. As it is not clear where these sites were actually located, any sites with duplicated coordinates were excluded from the processed CPT dataset. Additional criteria included removing any sites corresponding to non-applicable (primarily blank) QMAP units (see Section 2.2), and where there was poor coverage from the Riccarton Gravel and volcanic rock surfaces used to define the depths to these features (see Section 2.4). These latter sites were primarily located near the Port Hills where there are generally poor constraints on the underlying surfaces due to lack of data. All CPT sites with a maximum depth < 2 m located east of Fitzgerald Avenue, and all extreme spatial outliers (sites in Lyttelton, Akaroa, north of the Ashley River, and far to the west of Christchurch) were also excluded from the processed dataset. Based on the aforementioned exclusion criteria (see Fig. 2.1), a total of 10550 CPT sites were retained in the processed dataset (i.e., 3120 CPT records were removed).

Fig. 2.2 summarizes the characteristics of the processed CPT dataset, showing the distributions of depth, z; cone tip resistance, q_c; cone frictional resistance, f_s; and soil behaviour type index, I_c [24]. As shown, the majority of the data is for depths $z \leq 20$ m, cone tip resistances $q_c \leq 20$ MPa, and cone frictional resistances $f_s \leq 0.15$ MPa. The overwhelming majority of the CPT readings possess a soil behaviour type index in the clean to silty sand range ($1.31 \leq I_c \leq 2.05$), though there is a fair amount of coverage for soil behaviour type indices up to about $I_c = 3.0$.

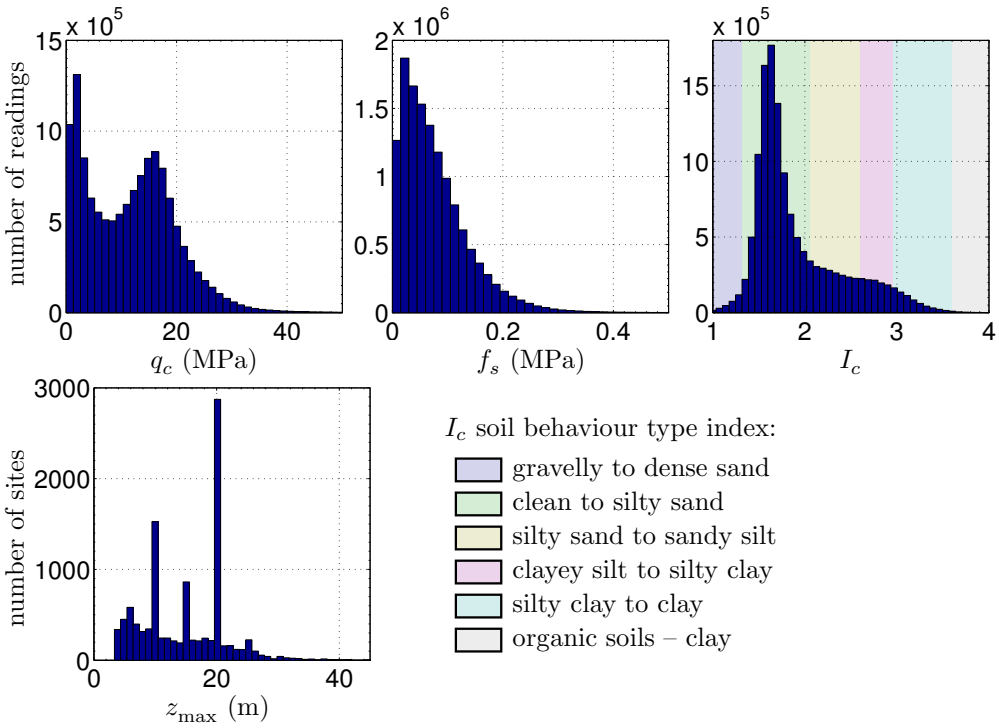

Fig. 2.2: Summary of CPT dataset showing distributions of depth, z, cone tip resistance, q_c, cone friction resistance, f_s, and soil behaviour type index, I_c.

2.1.2 Estimation of V_s from CPT data

Shear wave velocity profiles are estimated for each CPT record using the Christchurch-specific CPT-V_s correlation of McGann et al. [1, 2]

$$V_s(z) = Aq_c(z)^b f_s(z)^c z^d \tag{2.1}$$

where $A = 18.4$, $b = 0.144$, $c = 0.083$, $d = 0.278$, $q_c(z)$ and $f_s(z)$ are the cone tip and frictional resistances (units of kPa) at the depths, z, below the ground surface in meters. This empirical model was developed from sites located in the surficial Springston and Christchurch Formations, and is therefore not applicable to soil types not represented in these geologic units such as the loess soils found near the base of the Port Hills. As discussed in McGann et al. [1, 2], the CPT-V_s model can be used to characterize the uncertainty in the estimated V_s profiles; however, the focus here is given to the use of the mean correlation for a number of reasons. Firstly, the uncertainty in the model is small. Secondly, the emphasis in the current work is on region-wide estimation instead of site-specific characterization, and the CPT-V_s correlation is not only region-specific, but the range of CPT resistance readings and the associated soil behaviour types in the processed CPT dataset are consistent with those used in the development of the CPT-V_s model. Fig. 2.3 shows the distribution of the shear wave velocities estimated from the records of the adopted CPT dataset. As shown, the majority of the V_s values range between 80 m/s and 280 m/s, which is typical of Christchurch soils in the upper 20 m [e.g., 26, 27].

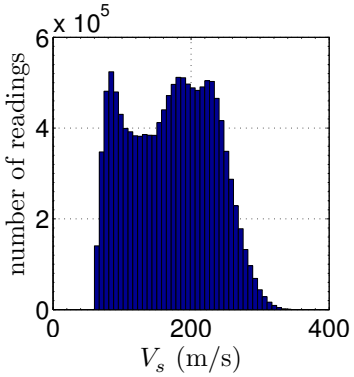

Fig. 2.3: Distribution of shear wave velocities estimated from CPT dataset.

2.2 General Geological/Geotechnical Characteristics of the Christchurch Region

The surficial soil deposits in the greater Christchurch urban area are primarily split between the beach, dune, coastal swamp, estuarine, and lagoonal deposits of the Christchurch Formation and the fluvial channel and overbank deposits of the Springston Formation [18]. The Christchurch Formation is primarily composed of blue gravel, sand, shells, sandy silts, clay, peat, and wood, and the Springston Formation soils are primarily gravels within a sand matrix interspersed with occasional silts and clays [28]. The Christchurch Formation is the predominant surface geology in the east adjacent to Pegasus Bay, with the Springston Formation to the west. As discussed by Begg et al. [29], the Christchurch Formation soils extend inland beneath the surficial Springston Formation soils about as far as the western edge of Hagley park, and this boundary is typically represented in CPT records as a noticeable change from variable to more homogeneous material properties occurring approximately at elevations corresponding to the present day sea level.

The 1:250,000 scale geologic map (QMAP) for Christchurch [30] data presented in Fig. 2.4 shows the layout of the various surficial geologic units in the area, which can be roughly grouped into four main units: alluvium, estuarine, marine, and peat/swamp. The soils in the ridges and valleys of the Port Hills to the south of Christchurch city differ from those in the plains below,

primarily consisting of loess and colluvium deposits. These surficial units are not considered in the current work as the Christchurch-specific CPT-V_s correlation is not applicable to the loess and colluvium soils [22]. Sites located in anthropic and active riverbed deposits are also ignored in subsequent development.

2.3 Groundwater Table Data

The depth of the groundwater table at each CPT site was obtained from information reported in the CPT logs. The median estimated groundwater elevation surface of van Ballegooy et al. [31], developed from long term ($\geq$ 12 months) observations at 657 monitoring wells, was used to supplement the data available in the CPT records for sites where no measured groundwater table depth was reported or where the reported water table depth did not correspond with surrounding readings. The groundwater data does not directly influence the shear wave velocities estimated from the CPT logs, as the CPT-V_s correlation of Eq. (2.1) is based on depth instead of vertical effective stress, but the groundwater data is used to compute vertical effective stress profiles used for the computation of various CPT-based parameters such as normalized tip resistances and soil behaviour type indices.

2.4 Riccarton Gravel and Banks Peninsula Volcanics Surfaces

The post-glacial Springston and Christchurch Formations that comprise the majority of the near-surface sediments in the Christchurch region are underlain by an alternating series of gravel layers deposited during periods of glaciation and non-gravel layers deposited during inter-glacial periods of elevated sea level [18]. The Riccarton Gravel Formation is the uppermost gravel layer of the series of interbedded gravels underlying the near-surface alluvial, estuarine, swamp, and marine deposits of the current post-glacial period. The Riccarton Gravel extends from the Canterbury plains west of Christchurch, where it is manifested on the ground surface, to the eastern edge of Christchurch and into Pegasus Bay, becoming deeper with to the east. For much of the region, the upper boundary of the Riccarton Gravel represents the most significant shear wave velocity contrast in the near-surface ($z < 40$ m) zone, therefore, the depth to the top of this layer is an important feature in the V_s profile (and V_{s30} value) for a given location. In the southern suburbs of Christchurch, which are located in the Port Hills on the northern rim of the extinct Lyttelton Volcano [18], the surficial sediments are often directly underlain by the volcanic rock of the Lyttelton Volcanic group and Mount Pleasant formation instead of the Riccarton Gravel, and the upper boundary of this volcanic surface is an equally important feature in the V_s profiles and corresponding V_{s30} values.

A pair of interpolated surfaces describing the elevations of the upper boundaries of the Riccarton Gravel and volcanic rock layers have been developed using several forms of constraints, including well log data from about 530 sites in the Canterbury region [3] and, for the Riccarton Gravel, the western outcrop of this surface per the GNS QMAP data for the Christchurch area [30]. These surfaces are used to estimate the depth to the top of the Riccarton Gravel or volcanic rock layers at each CPT site. For sites where the CPT termination depth is deeper than the estimated depth to these surfaces, the termination depth is used. The Riccarton Gravel and volcanic rock surfaces (modified based on CPT termination) are shown using contour lines in Fig. 2.4. As shown, the upper boundary of the Riccarton Gravel is shallower ($\approx$ 15 m below the surface) in the western parts of the Christchurch area and increases in depth moving east (up to about 40 m deep near the coast). The areas where the volcanic rock surface is more shallow than the Riccarton Gravel are confined to the immediate vicinity of the Port Hills.

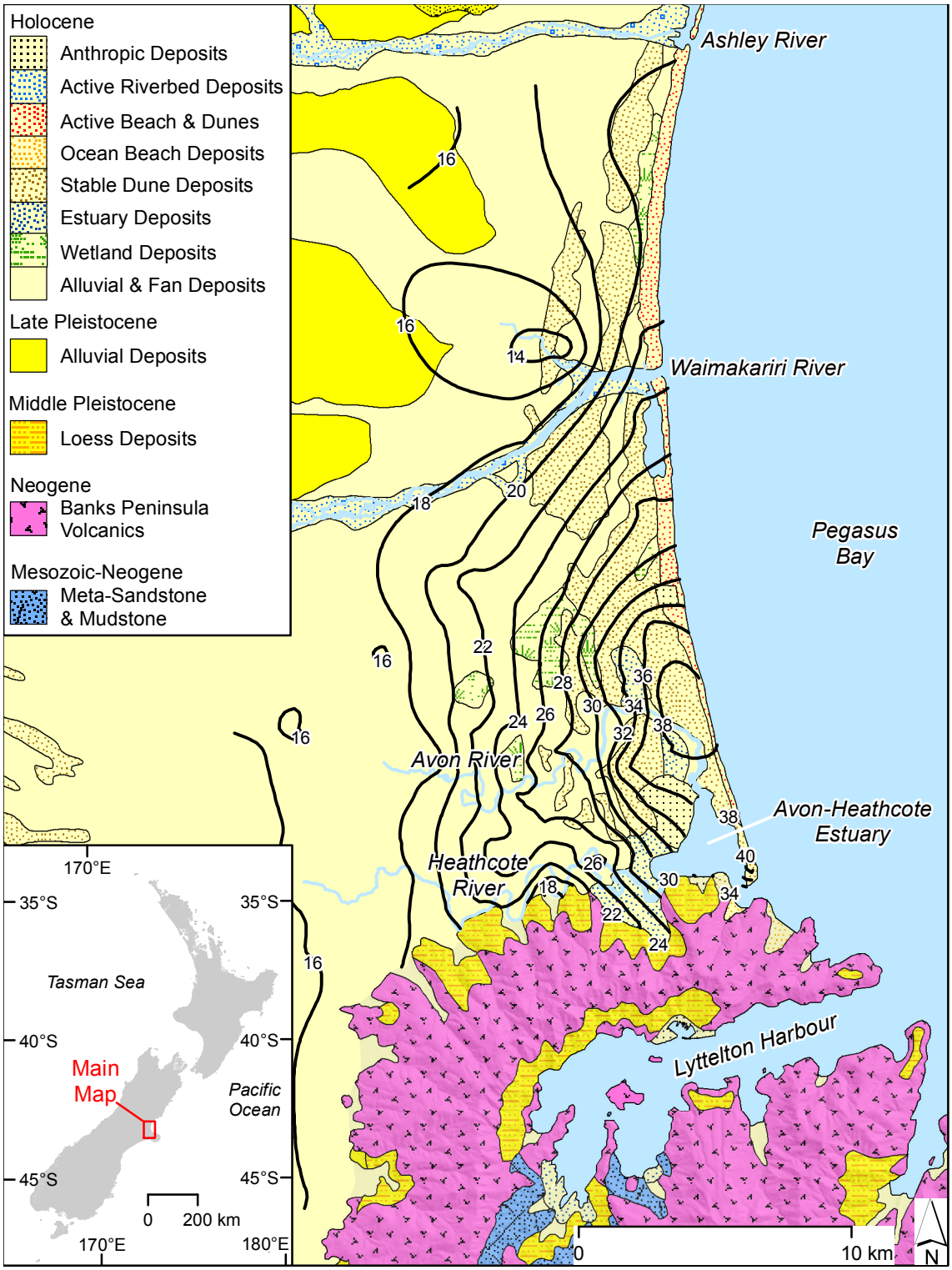

Fig. 2.4: Surficial geology of Christchurch region with contours showing depth (in meters) to the top of the Riccarton Gravel and/or volcanic rock surfaces underlying the Holocene sediments. Contour lines are spaced on 2 m intervals.

2.4.1 Estimation of V_s in gravel and volcanic rock layers

The computation of V_{s30} at a particular location equires the estimation of V_s values for the Riccarton Gravel and volcanic rock layers for sites where the upper boundaries of these surfaces are located at depths less than 30 m. Shear wave velocities for the Riccarton Gravel are estimated using the dense gravel reference V_s profile suggested by Lin et al. [32]. This reference profile corresponds to a dense gravel with relative density, $D_r = 95\%$, median grain diameter, $D_{50} = 5.0$ mm, and a uniformity coefficient, $C_u = D_{60}/D_{10} = 35$, and can be defined as

$$V_s = A_s \left(\frac{\sigma'_v}{p_a} \right)^n \tag{2.2}$$

where $A_s = 312$ m/s, $n = 0.331$, σ'_v is the vertical effective stress, and p_a is the atmospheric pressure in the same units as σ'_v. The effective stress profiles at each site are estimated using a soil density $\rho = 1.8$ Mg/m^3 and the estimated groundwater table depth at that location. The shear wave velocity of the volcanic rock is assumed to be a constant 750 m/s with depth within the layer. These gravel and rock velocity profiles are appended to the end of the CPT-V_s profile at each CPT site, up to a depth of 30 m. Fig. 2.5 shows 30 m deep velocity profiles for sites underlain by each surface type. The Riccarton Gravel site of Fig. 2.5(a) includes an indication of the V_s profile obtained from Eq. (2.2) (dashed line) to illustrate the difference between the CPT-based and assumed V_s across the full 30 m profile, though the portion of the gravel velocity profile below the estimated Riccarton Gravel surface depth (about 23 m at this site, depicted as solid line) is used in subsequent computations.

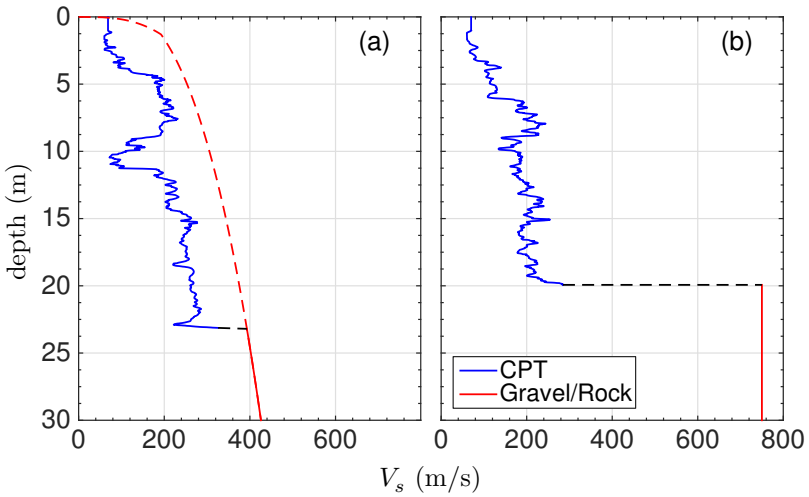

Fig. 2.5: Example 30 m V_s profiles including CPT-based V_s values and assumed V_s values for depths within underlying surfaces. (a) Site underlain by Riccarton Gravel. (b) Site underlain by volcanic rock.

2.5 Fill-in Interpolation for CPT-V_s Profiles

Only a small portion of the processed CPT records (about 550 out of 10550) were terminated at the upper boundaries of the Riccarton Gravel and volcanic rock surfaces. At the approximately 10000 sites remaining, the portion of the V_s profile between the end of the CPT and the top of the underlying gravel/rock surface cannot be directly obtained from the given CPT record. A fill-in technique based on spatial interpolation was adopted in order to increase the utility of

these incomplete V_s profiles. Interpolated surfaces of V_s were generated on 0.5 m depth intervals up to a depth of 30 m from all of the CPT-based V_s profiles that have data at each depth interval. The portion of each CPT-V_s profile between the termination depth and the top of the underlying gravel/rock surface was then filled-in with values queried from these interpolated surfaces.

This profile fill-in technique is evaluated by comparing the V_{s30} values at the 554 sites that did not require fill-in (fill-in length = 0 m) to the corresponding V_{s30} values returned by four allowable profile fill-in lengths: 3, 6, 10, and 15 m. This comparison is made at the grid points of an interpolated surface fit to the V_{s30} values for each case. The interpolation grid uses 200 × 200 m spacing, and all grid points are within 300 m of the 554 zero fill-in CPT sites. Fig. 2.6 shows the results of these comparisons with the zero fill-in values ($V_{s30}^{0\text{m}}$) on the vertical axes and the corresponding V_{s30} values for each allowable fill-in length on the horizontal axes. The coefficients of determination, r^2, and number of sites corresponding to each fill-in length, n, are indicated for each case.

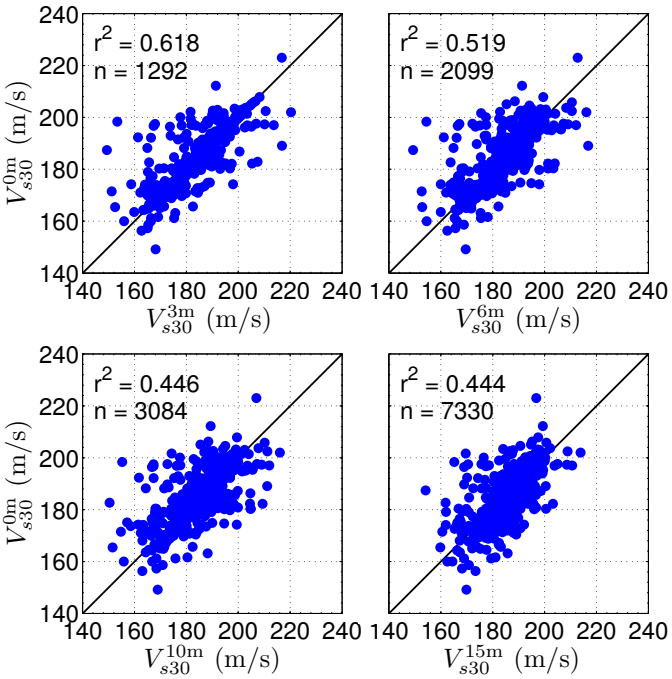

Fig. 2.6: Comparison of V_{s30} values for four allowable V_s profile fill-in lengths (3, 6, 10, 15 m) to zero fill-in length results. Number of sites, n, indicates the number of CPT sites that meet the allowable fill-in length criteria for each case (e.g., 1292 sites meet the 3 m fill-in criteria).

As the allowable fill-in length increases from 3 to 15 m, the degree of correlation to the zero length (i.e., 'exact') cases decreases from 0.618 to 0.444, while the number of CPT sites can be used in the computation of V_{s30} increases from $n = 1292$ to $n = 7330$. Though the degree of correlation with the zero fill-in cases is lowest for the 15 m allowable length, the overall error for this case evidenced in Fig. 2.6 is not substantially greater than the shorter allowable lengths. The allowable fill-in length criteria applied to the CPT dataset for the computation of time averaged shear wave velocities to various target depths (e.g., V_{s5}, V_{s30}) is based on the 15 m allowable length case. For each CPT record, the fill-in length is restricted to be $\leq 50\%$ of the lessor of the depth to the top of the underlying gravel/rock surface or the target depth of the time averaged profile. As the deepest profile considered is 30 m, this restricts the maximum acceptable fill-in length to 15 m, though for most sites a lesser length was used.

Chapter 3

Development of V_{sz} Surfaces for Christchurch Urban Area

The CPT dataset documented in the previous chapter is used to develop surfaces describing the distribution of time-averaged shear wave velocity, V_{sz}, across the greater Christchurch urban area. Target profile depths of $z = 5$, 10, 20, 30 m are considered to allow for an assessment of the distributions of soil stiffness with depth across the region. V_{sz} values are computed for each target depth, z, as

$$V_{sz} = \frac{\sum d_i}{\sum (d_i / V_{si})} \tag{3.1}$$

where d_i are CPT depth measurement increments up to the target depth, and V_{si} are mean shear wave velocities over each measurement increment determined from the Christchurch-specific CPT-V_s correlation of McGann et al. [1, 2]. The V_{sz} values determined at the CPT sites are used to generate interpolated surfaces that extend the spatial scope of the results. The resulting surfaces are used to gain insights into the spatial distribution of near-surface soil stiffness in the region, and to comment on the applicability of such measures as predictors/descriptors of site response and tools for site classification in the Christchurch area (via comparison with observed response to the 2010-2011 Canterbury earthquakes).

3.1 Spatial Interpolation for V_{sz} Surfaces

Smooth surfaces of V_{sz} that approximate the CPT-based V_{sz} data points determined using Eq. 3.1 were fit to 200 × 200 m grids. If no CPT record was within 300 m of a single grid point, then no estimate of V_{sz} was computed. This 300 m boundary was selected based on an examination of the spatial variability in the soil profiles, and was enforced to ensure the resulting surfaces focus only on well-constrained estimates as opposed to estimates over the full urban region. Users who desire estimates in areas not considered here could make crude assumptions of interpolation between areas with presented data, or preferably, obtain V_s profiles directly from site-specific CPT data. Each grid is subdivided according to the surficial geologic units (QMAP units) indicated on the 1:250,000 scale geologic map (QMAP) of Christchurch [30] (see Fig. 2.4), and for each target depth, z, the full V_{sz} surface is compiled from separate surfaces fit to the CPT results located in the alluvium, marine/dune, estuarine, and peat/swamp QMAP units to avoid interpolation or extrapolation across surficial geologic boundaries. The surface-fitting procedure uses a modified ridge estimator [33] that is biased towards smoothness to achieve surfaces that are representative of the trends in the CPT results without necessarily representing V_{sz} at any particular site. The level of smoothness for each QMAP unit and target depth was selected to provide the best representation of the corresponding CPT results without becoming overly bumpy, and the surfaces are regularized such that extrapolation is minimized.

3.2 V_{sz} Surfaces

Figs. 3.1, 3.3, 3.5, and 3.7 show the values of V_{sz} (for $z = 5$, 10, 20, and 30 m, respectively) computed from the CPT dataset and plotted at the CPT locations, while Figs. 3.2, 3.4, 3.6, and 3.8 show the corresponding results for the developed surfaces. For reference, major roads are indicated as black lines, and locations of a number of Christchurch suburbs and surrounding towns are indicated in the fitted surface for most cases. The colour of the markers indicates the magnitude of V_{sz} at a given location, and the extents of the V_{sz} scale in each map are adjusted to best represent each respective target depth. Horizontal and vertical axes indicate the distance in kilometers from the lower-left datum.

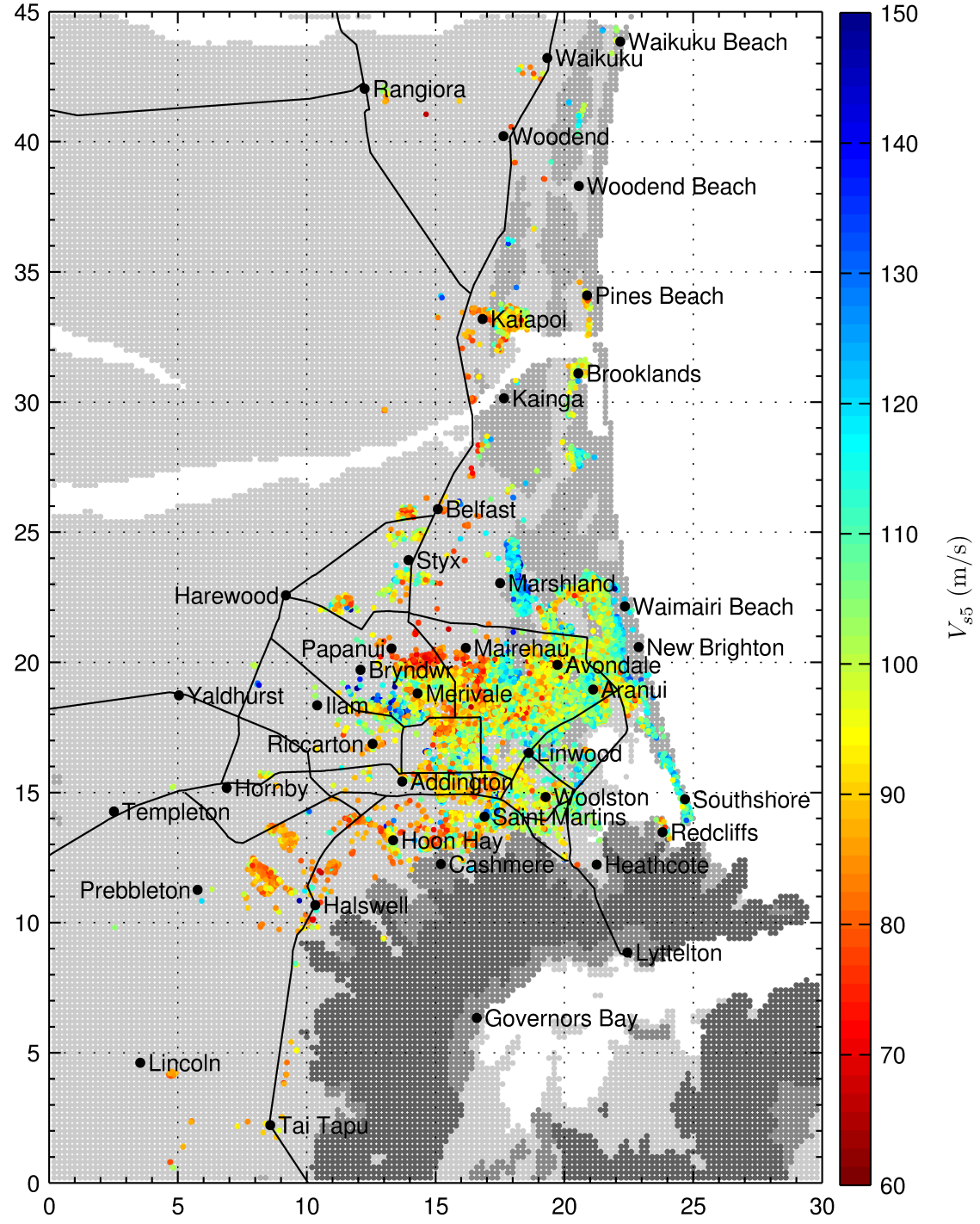

Fig. 3.1: V_{s5} at CPT sites. NZMG projection; horizontal and vertical axes indicate km from lower left corner of map. Latitude/Longitude (WGS84) bounds for the map are (−43.6811°, 172.4418°) and (−43.2773°, 172.8151°).

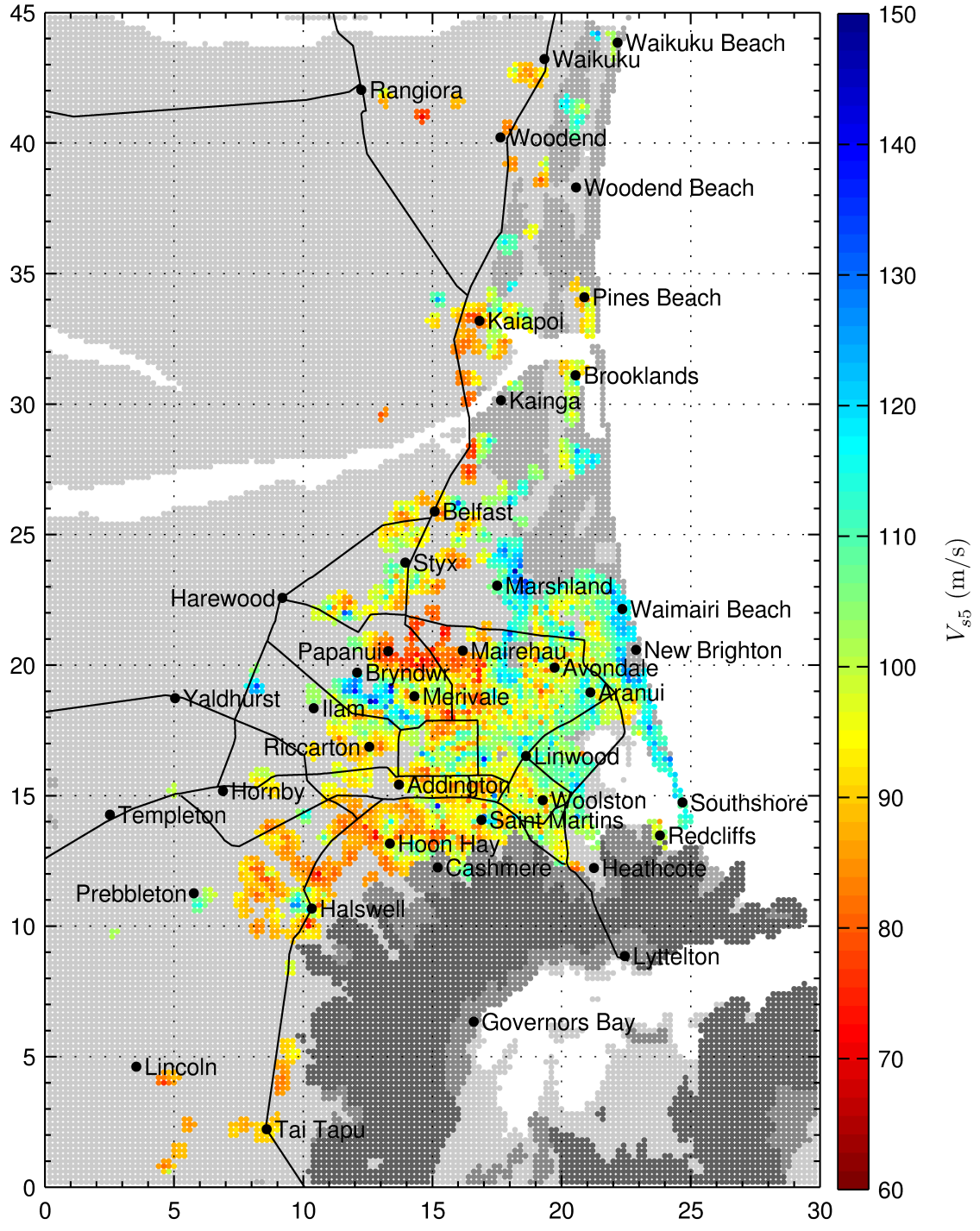

Fig. 3.2: V_{s5} surface on uniform 200 × 200 m grid. NZMG projection; horizontal and vertical axes indicate km from lower left corner of map. Latitude/Longitude (WGS84) bounds for the map are (−43.6811°, 172.4418°) and (−43.2773°, 172.8151°). Predictions are only provided in each grid cell if there is one or more CPT record within 300 m.

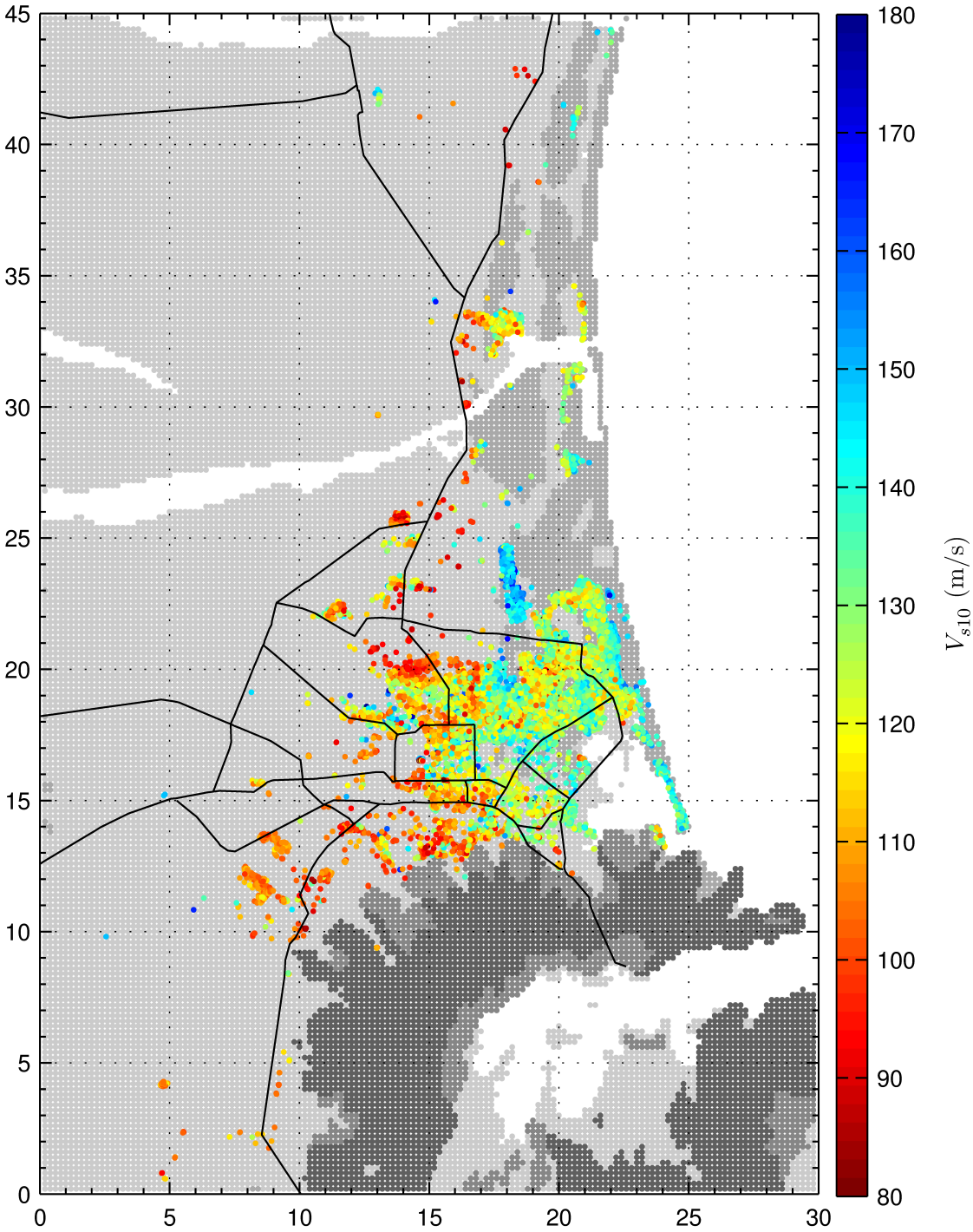

Fig. 3.3: V_{s10} at CPT sites. NZMG projection; horizontal and vertical axes indicate km from lower left corner of map. Latitude/Longitude (WGS84) bounds for the map are (−43.6811°, 172.4418°) and (−43.2773°, 172.8151°).

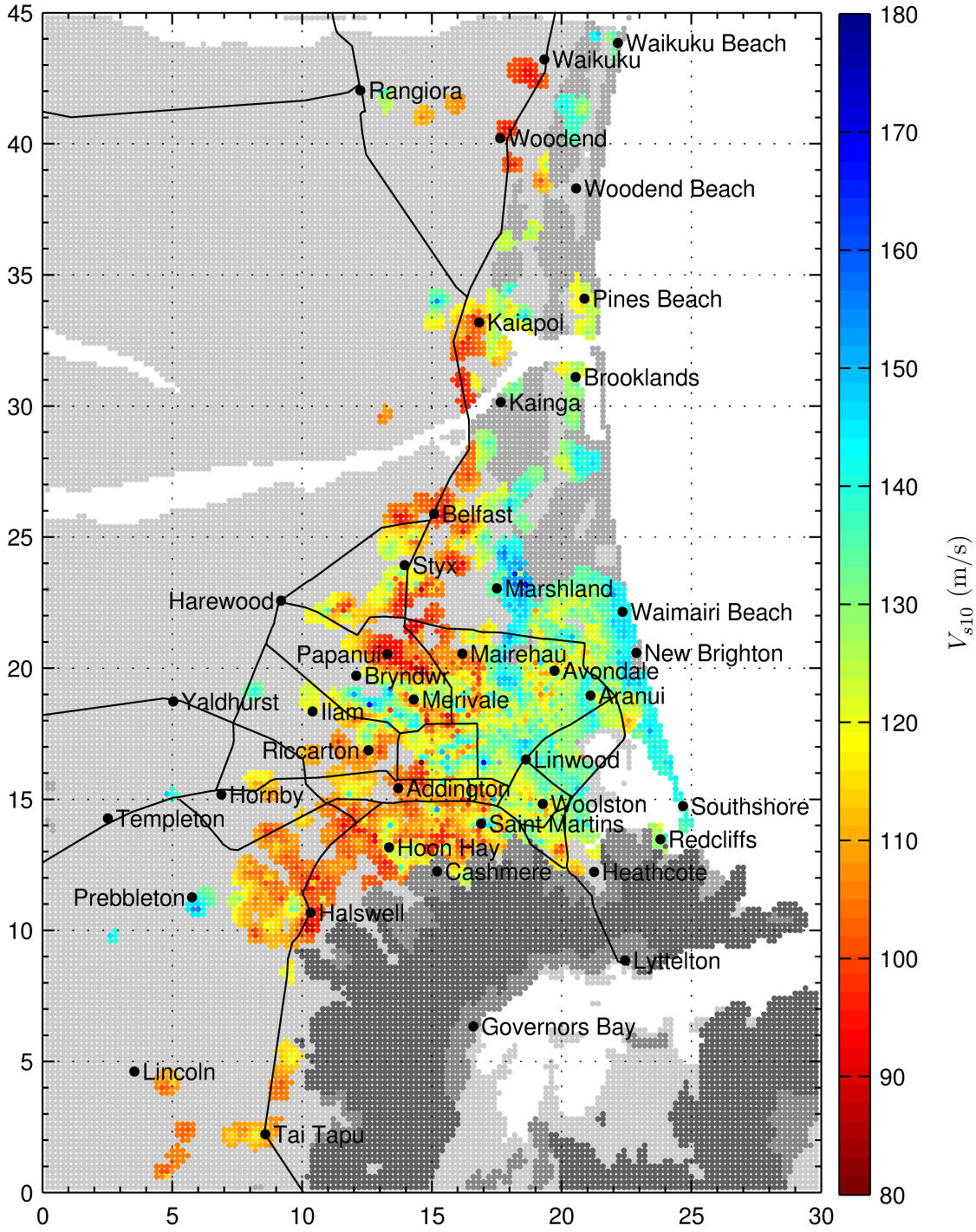

Fig. 3.4: V_{s10} surface on uniform 200 × 200 m grid. NZMG projection; horizontal and vertical axes indicate km from lower left corner of map. Latitude/Longitude (WGS84) bounds for the map are (−43.6811°, 172.4418°) and (−43.2773°, 172.8151°). Predictions are only provided in each grid cell if there is one or more CPT record within 300 m.

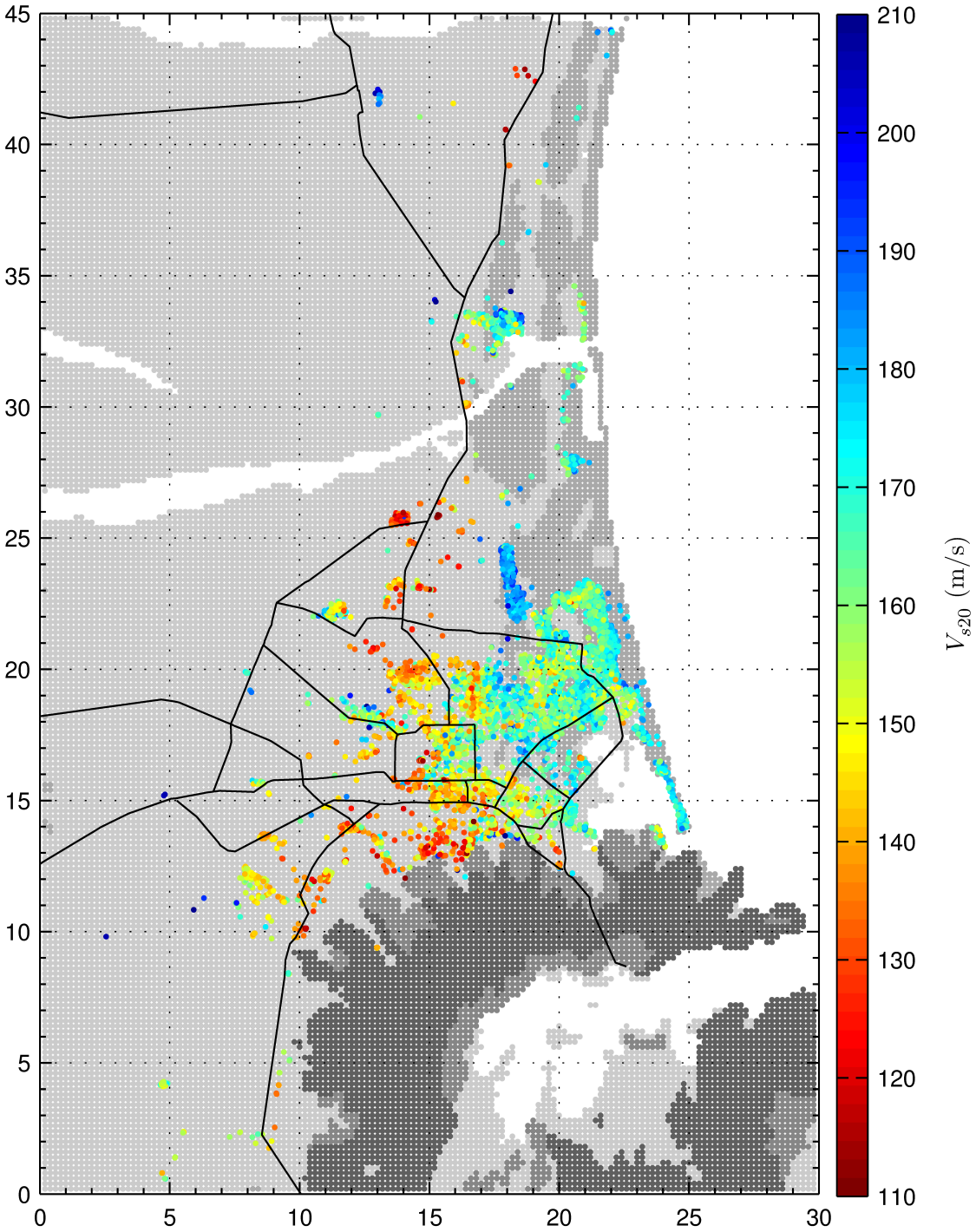

Fig. 3.5: V_{s20} at CPT sites. NZMG projection; horizontal and vertical axes indicate km from lower left corner of map. Latitude/Longitude (WGS84) bounds for the map are (−43.6811°, 172.4418°) and (−43.2773°, 172.8151°).

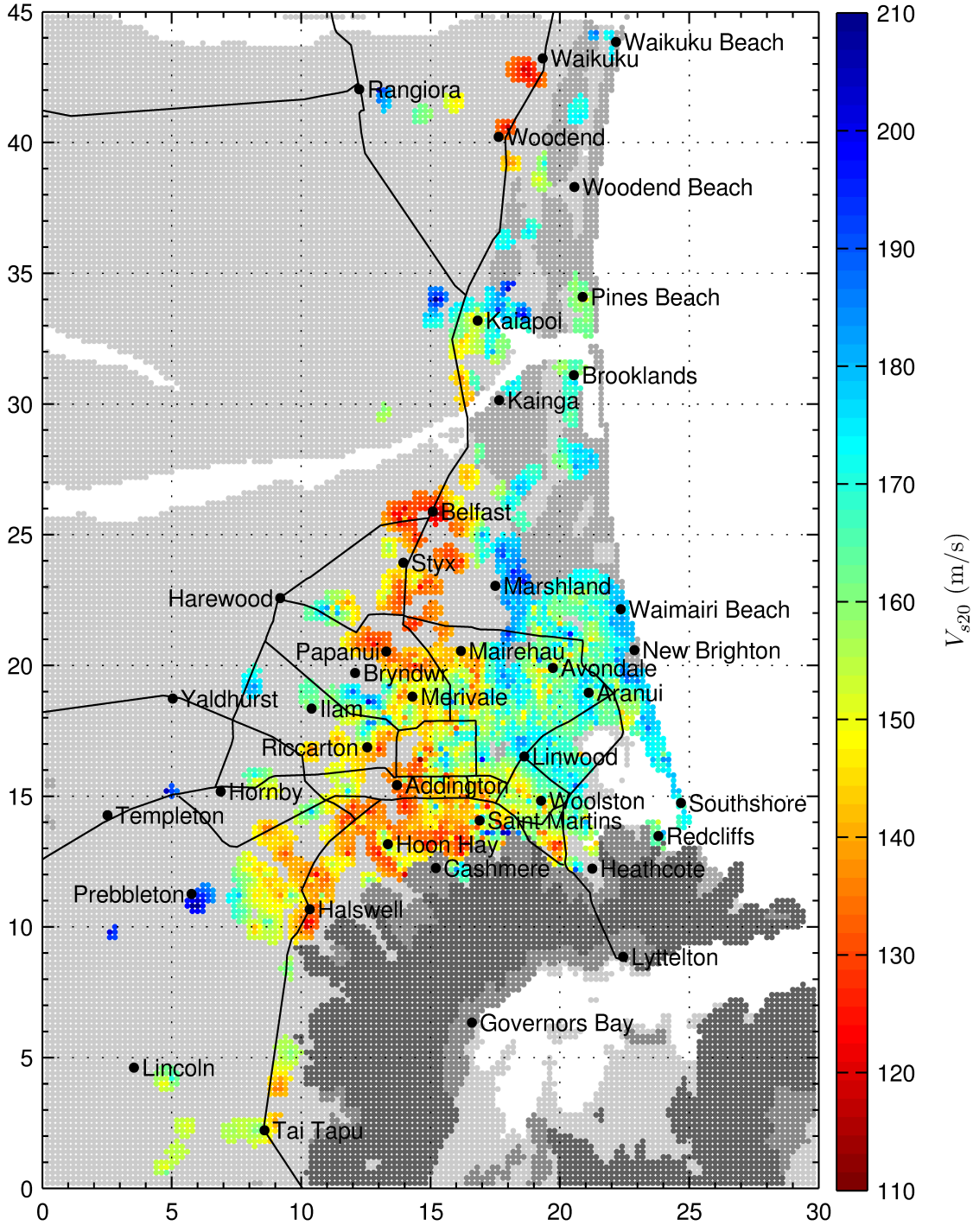

Fig. 3.6: V_{s20} surface on uniform 200 × 200 m grid. NZMG projection; horizontal and vertical axes indicate km from lower left corner of map. Latitude/Longitude (WGS84) bounds for the map are (−43.6811°, 172.4418°) and (−43.2773°, 172.8151°). Predictions are only provided in each grid cell if there is one or more CPT record within 300 m.

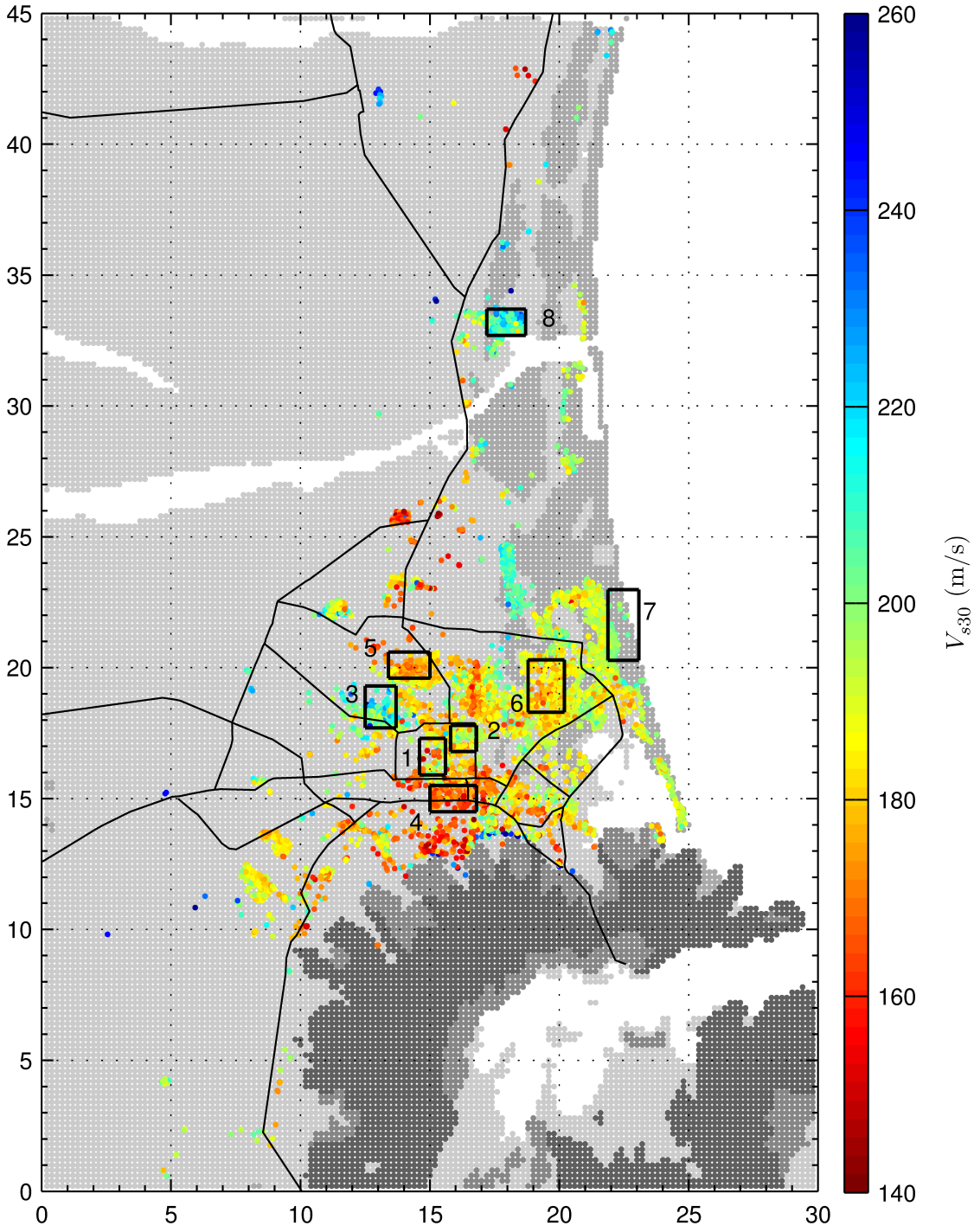

Fig. 3.7: V_{s30} at CPT sites. NZMG projection; horizontal and vertical axes indicate km from lower left corner of map. Latitude/Longitude (WGS84) bounds for the map are (−43.6811°, 172.4418°) and (−43.2773°, 172.8151°). The numbered regions enclosed in black boxes refer to the subregions of Chapter 4.

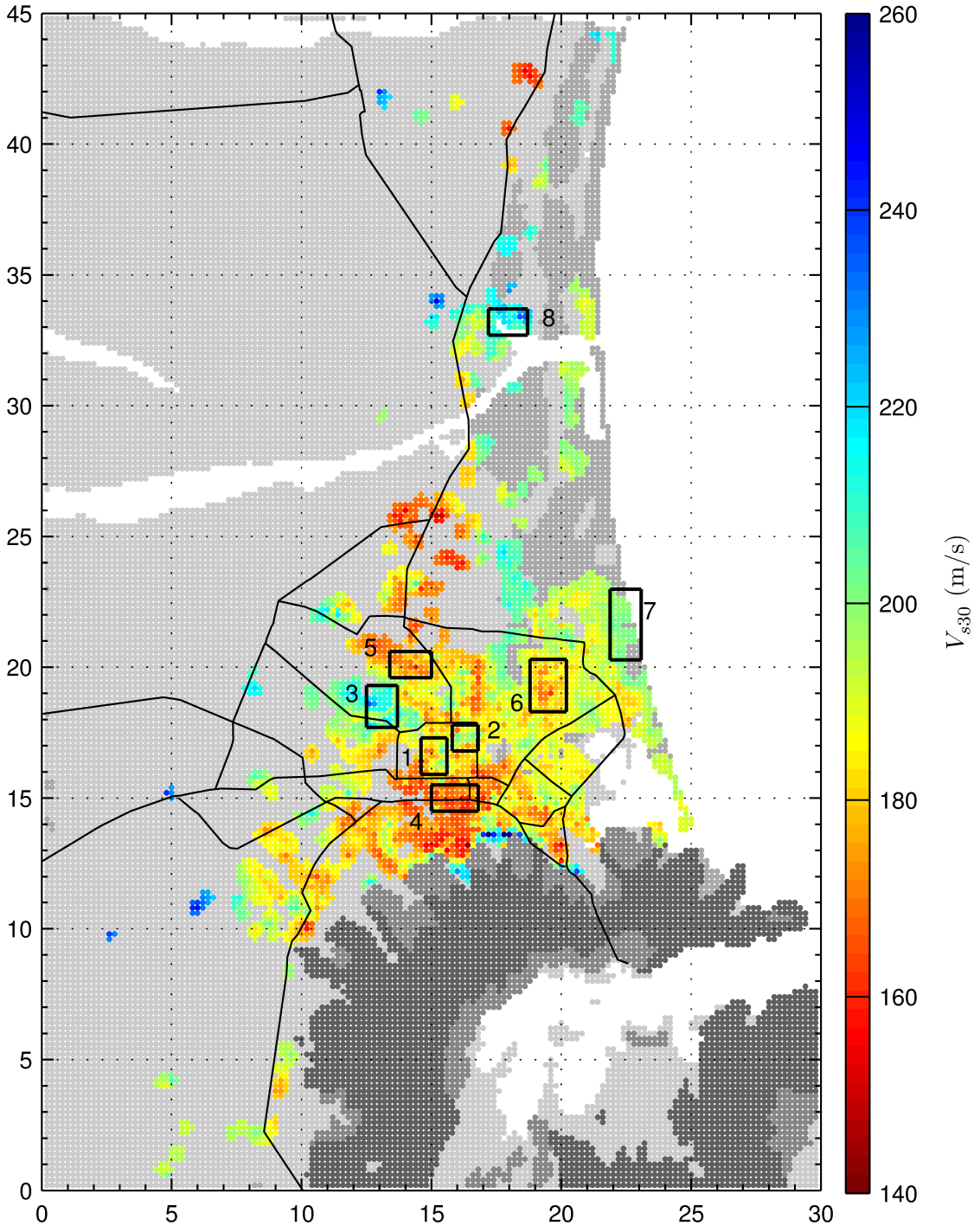

Fig. 3.8: V_{s30} surface on uniform 200 × 200 m grid. NZMG projection; horizontal and vertical axes indicate km from lower left corner of map. Latitude/Longitude (WGS84) bounds for the map are (−43.6811°, 172.4418°) and (−43.2773°, 172.8151°). Predictions are only provided in each grid cell if there is one or more CPT record within 300 m. The numbered regions enclosed in black boxes refer to the subregions of Chapter 4.

As shown in Figs.3.1-3.8, there is a large degree of spatial variability in V_{sz}, with values varying by about 100-120 m/s for each target depth. For all cases, with the exception of some western sites with shallow gravels, there is a general trend of increasing V_{sz} from west to east, as the values within the marine/dune QMAP unit located in the east tend to be higher than those in the alluvial, peat/swamp, and estuarine units located further west. The increased velocities in the marine/dune deposits may be due a combination of densification due to wave-action during deposition and the relative lack of fines and plastic soils in these deposits in comparison to the other surficial units. The general band of softer alluvial sites located between Belfast in the north and the Port Hills in the south, in particular, have an increased amount of silty and clayey soil relative to the rest of the region, and the eastern edge of this soft band, extending southeast from about (17,20) to (22,14) in the coordinates noted in Figs.3.1-3.8, roughly corresponds with the coastline that existed approximately 3000 years ago [18, (Fig. 7)].

The sites located at the toe of the Port Hills to the south of Christchurch city display some of the highest V_{s30} values for the region, as these sites are generally underlain by volcanic rock at shallow (< 30 m) depths, as opposed to the Riccarton Gravels below the remainder of the sites. As the Banks Peninsula Volcanics is assigned a 750 m/s shear wave velocity, the presence of the volcanic interface in the upper 30 m results in significantly higher V_{s30} values than are possible elsewhere. The fill-in criteria specified to account for sites that did not terminate directly at the interface with the volcanics surface creates a slight bias towards increased V_{s30} in these areas, as typically only the sites with relatively shallow rock surfaces (somewhere between 10 and 20 m) meet the fill-in criteria. While this is generally true for the entire dataset, the relative scarcity of sites that are underlain by the volcanics increases the visibility of this bias. The other areas that have notably increased values of V_{s30} include the surficial dune sands in the east, which are clearly visible on the coast and the immediate western side of the estuary near Aranui, and some of the Springston Formation over-bank deposit lobes in the western part of the city [18, Figs. 15 and 49]. One such lobe is visible as the blue path between Ilam, Merivale, and Bryndwr, while others are notable for their absence from the surfaces (i.e., no CPT data for surficial gravels).

The maps presented Figs.3.1-3.8 for different depths provide different insights into the characteristics and expected seismic responses for different regions within the Christchurch area. Profiles in locations with lower values of V_{s5} and V_{s10} may be relatively soft on average over the full 30 m in comparison to the entire region (e.g., Papanui and Sydenham) or may be relatively stiff on average (e.g., Kaiapoi and parts of Halswell) due to changes in the soil profile occurring below 10 m. The V_{sz} surfaces developed for the different target profile depths are useful for different purposes, with no one single surface providing the means with which to fully-characterize the expected seismic response of a particular site. The surfaces for the shallower target depths, V_{s5} and V_{s10}, provide a characterization of the very-near-surface soils in the upper 5-10 m below the ground surface that, in combination with soil behaviour type or borelog data, can be useful for assessing liquefaction susceptibility. The surfaces for the deeper target depths, V_{s20} and V_{s30}, provide a general idea of how a particular site may respond in an overall sense during earthquake shaking.

3.3 Assessment of V_{s30} Surface Quality

A visual comparison of the results shown in Figs. 3.1-3.8 indicates that the smoothened V_{sz} surfaces are representative of their respective underlying CPT-based point data. For the sake of brevity, and because the V_{s30} results are representative of all four considered target depths, the distributions of V_{s30} computed at the CPT locations and at the interpolated grid points are considered in further detail to provide a quantifiable assessment of the quality of fit provided by these surfaces. It is important to again note that outer edges of the V_{sz} surfaces (and any edge bordering an area without data) are less constrained than the interior portions of the

surfaces. Grid points were included in the fitted surfaces only if they were within 300 m of a CPT location to limit the amount of edge extrapolation, however, extrapolation may still occur over this allowable distance. Values on the edges of the V_{sz} surfaces should therefore be treated with less confidence than interior areas, and it is beneficial to consult the corresponding map of V_{sz} plotted at the CPT sites to qualitatively assess such locations.

Fig. 3.9 shows the distributions of V_{s30} at the CPT sites and the grid points of the fitted surface. The distributions of V_{s30} for the two cases are well represented by normal distributions and, as shown in Fig. 3.9 and the final row of Table 3.1, the two cases are similar in terms of mean values (μ_{CPT} and μ_{surface} for the CPT sites and fitted surfaces, respectively) and variance (standard deviation, σ, and coefficient of variation, COV), demonstrating that the fitted surface captures the CPT-based data well in an overall sense. Table 3.1 also separately lists the normal distribution parameters for the CPT sites located within the four considered QMAP surficial geologic units and the corresponding subsurfaces for these units that were compiled into the overall V_{s30} surface. As shown, the subsurfaces associated with each QMAP unit are also representative of the corresponding subsets of the CPT dataset in an overall sense.

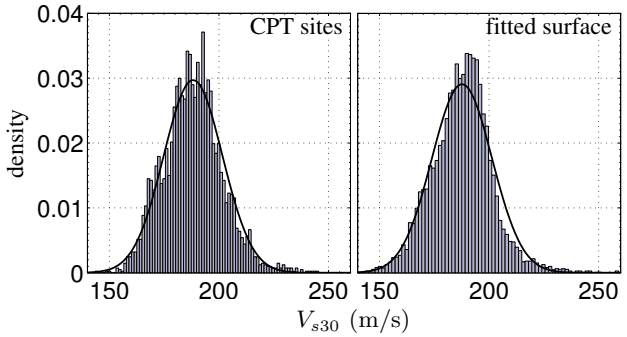

Fig. 3.9: Distributions of V_{s30} at CPT sites and grid points of 200 × 200 m surface. The parameters of the approximate normal distributions are provided in Table 3.1.

It is interesting to note the differences in the nature of the soils contained within the considered QMAP units revealed by the normal distribution parameters of Table 3.1. The marine/dune deposits have higher V_{s30} values on average than the other deposits (though the differences are relatively small), perhaps due to wave-action-based densification, and also display less variance, indicating a greater level of homogeneity in comparison to the other units. The alluvial deposits show the largest amount of variance, which is consistent with expectations as this is the largest and most varied of the four considered units. These differences in character between the QMAP units support the decision to generate the overall V_{sz} surfaces as a set of subsurfaces that consider only the CPT sites within each QMAP unit. The generation of a single surface without regard to the surficial geology of the considered sites may have led to interpolation/extrapolation across unit boundaries, potentially obscuring some of the natural spatial variability of the region.

Table 3.1: Mean, standard deviation, and coefficient of variation for V_{s30} at CPT sites and surface grid points for QMAP units and overall dataset.

QMAP Unit	μ_{CPT}	μ_{surface}	σ_{CPT}	σ_{surface}	COV_{CPT}	$\text{COV}_{\text{surface}}$
alluvium	184.3	186.0	15.52	17.52	8.42%	9.42%
marine/dune	192.6	196.3	8.56	9.68	4.44%	4.93%
estuarine	187.9	185.2	10.05	10.24	5.35%	5.53%
peat/swamp	190.3	193.0	15.43	14.43	8.08%	7.48%
all data	187.6	188.2	13.73	13.44	7.32%	7.14%

Fig. 3.10 compares the North-South and East-West spatial variability in V_{s30} at the CPT locations and the surface grid points (red and blue markers, respectively) by plotting the moving averages (solid lines) for the two cases with their associated 95% confidence intervals (dashed lines). The North-South and East-West variability shown at left and right, respectively, and the distance scales correspond to those in the V_{sz} maps of Figs. 3.1 through 3.8. As shown in Fig. 3.10, the smoothened V_{s30} surface generally captures the average spatial trends evident in the CPT results, and the confidence intervals for the two cases are nearly coincident, especially in the data-rich areas away from the extents of the CPT dataset.

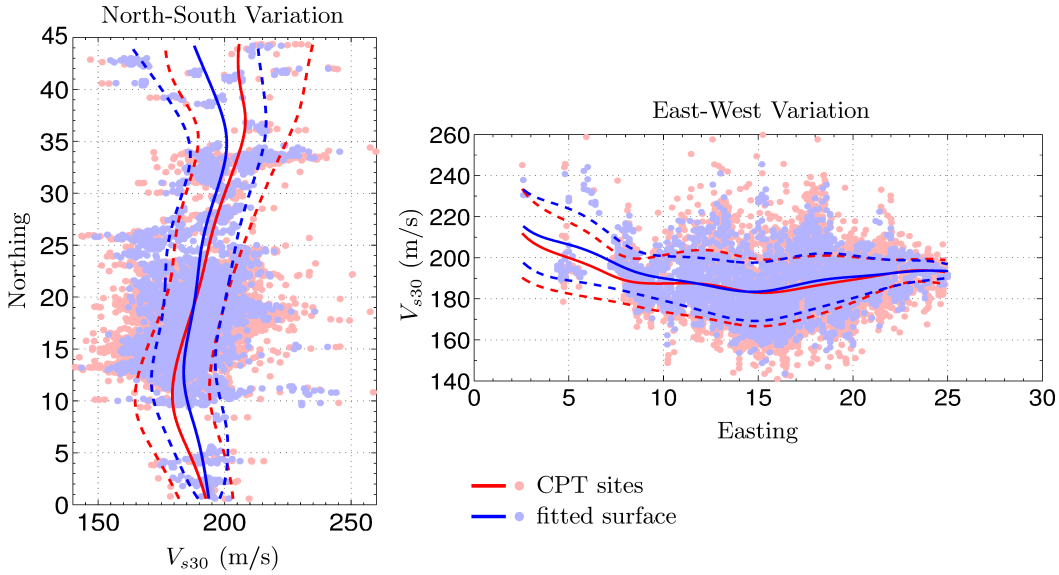

Fig. 3.10: North-South and East-West spatial variability in V_{s30} for CPT sites (red lines and markers) and grid points in the surface (blue lines and markers). Solid and dashed lines indicate running average with 95% confidence intervals.

The results shown in Figs. 3.9 and 3.10 and Table 3.1 provide strong support for the adequacy of the smoothened surfaces in representing the spatial variation in V_{sz} suggested by the CPT dataset. The V_{s30} surface captures well the mean and variance of the CPT results for the entire dataset and within each QMAP unit, and also captures the spatial variation inherent in the CPT results. This spatial variability is explored further in the following chapter through the development of typical shear wave velocity and soil behaviour type index profiles for different subregions within the greater Christchurch urban area.

3.4 Observed Correlation Between V_{s30} and V_{sz}

Fig. 3.11 compares the V_{s30} values at the grid points of the fitted surface with corresponding values returned for target depths $z < 30$ m; and Table 3.2 provides the coefficients of determination, r^2, between V_{sz} and V_{s30}, with separate values for the full dataset and the sites within each QMAP unit comprising the full set. Two additional target depths ($z = 15$, 25 m) were considered to provide an assessment of the correlation between V_{s30} and V_{sz} at 5 m intervals. As shown, the degree of correlation between V_{sz} and V_{s30} differs depending on the QMAP units of the Christchurch sites. For sites in the alluvial, marine/dune, and estuarine QMAP units that comprise the majority of the overall data set, there is little correlation between V_{s5} and V_{s30}, and the degree of correlation between V_{sz} and V_{s30} generally increases with profile depth. A much stronger correlation is observed for all profile depths in the peat/swamp sites, especially relative to the other QMAP units. This increased correlation is likely due to the soil profiles of the peat/swamp sites, which are often characterized by relatively thick layers of low V_s soils near the ground surface that substantially affect, and tend to homogenize, V_{sz} values due to their prominence in the profiles.

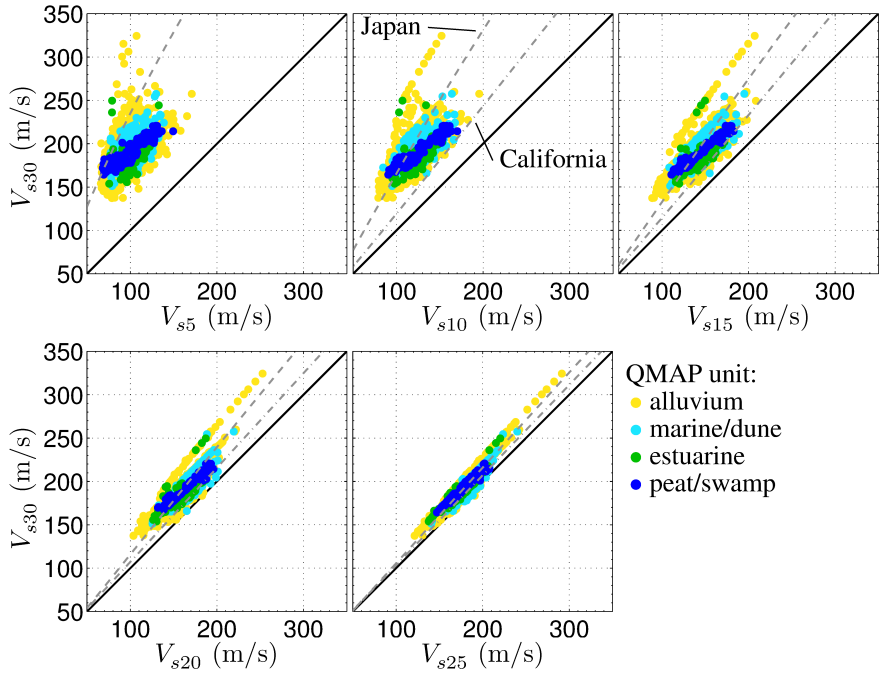

Fig. 3.11: Comparison of V_{sz} with V_{s30} for z = 5, 10, 15, 20, 25 m. Marker colour indicates surficial QMAP geologic unit. Dot-dashed and dashed lines indicate regression models of Boore [34] and Boore et al. [35], respectively (data not available at 5 m depth in [34]).

Table 3.2: Coefficients of determination, r^2, between V_{sz} and V_{s30} for QMAP units and overall dataset.

QMAP Unit	V_{s5}	V_{s10}	V_{s15}	V_{s20}	V_{s25}
alluvium	0.34	0.45	0.58	0.76	0.93
marine/dune	0.45	0.58	0.68	0.76	0.86
estuarine	0.35	0.44	0.57	0.74	0.92
peat/swamp	0.85	0.91	0.95	0.95	0.96
all data	0.41	0.51	0.63	0.77	0.91

The lack of correspondence between V_{s30} and V_{sz} for shallow z in the non-peat/swamp sites is inferred as a result of the stratified nature of the soils underlying the Christchurch region. As shown in Fig. 2.4, the upper boundary of the Riccarton Gravel that underlies most of the region is $<$ 30 m below the ground surface. For a given site, the shear wave velocity of the Riccarton Gravel is both independent of, and much larger than, that in the overlying soils, therefore, V_{sz} values for depths above the Riccarton Gravel will not correspond to velocities averaged over the entire 30 m profile. The relationship between the depth to the Riccarton Gravel and the degree of correlation between V_{sz} and V_{s30} is evident in the spread in the data points for the alluvium and marine/dune sites in the V_{s5} and V_{s10} plots of Fig. 3.11. The sites that plot nearer the 1:1 correlation line are those sites where the Riccarton Gravel is likely deep, and the sites that plot nearer the left-hand edge of the plots are likely those where the Riccarton Gravel is shallow. In effect, for the alluvium and marine/dune sites, moving from left to right across the data points (for a given y-axis value) in the V_{s5} subplot of Fig. 3.11 represents a move from west to east across Christchurch.

The V_{s30} values estimated by two V_{sz} prediction models [34, 35] are added to Fig. 3.11 for reference. The dot-dashed lines show the results for the Boore [34] model developed using V_s profile data from strong-motion stations in California (model not applicable to V_{s5}), and the dashed lines show the results for the Boore et al. [35] model developed using V_s profile data from boreholes at Kiban-Kyoshin Network (KiK-net) stations in Japan. As shown, the Japan-based

model is more representative of the Christchurch data than the California-based model, which tends to estimate lower V_{s30} values for a given value of V_{sz}, likely due to the composition of the soil profiles and soil types represented by the California, Japan, and Christchurch datasets. The California stations were primarily sited in the Los Angeles and San Francisco areas, which are typically underlain by sedimentary basins that are relatively uniform in nature in the first 30 m below the ground surface; subsurface conditions not representative of those in Christchurch. In contrast, the V_{s30}-V_{sz} correlations for the KiK-net data are from locations throughout the entire Honshu region of Japan and thus represent a larger variety of soil conditions. The Japanese sites include areas of shallow sediment over rock that are more similar in nature to the conditions in Christchurch. The differences in the degree of correlation between V_{s30} and V_{sz} both in terms of regional data (California, Japan, Christchurch) and surficial geologic unit (e.g., peat/swamp or alluvial deposits) highlights the importance of consideration for the one prevalent soil type or layer (low or high V_s) that controls the velocity profile when computing V_{s30}.

3.5 Site Classification from V_{sz} Surfaces

One application of V_{s30} that is widely used for site characterization purposes is the definition of V_{s30}-based site classes, e.g., United States National Earthquake Hazards Reduction Program (NEHRP) site classes [11, 12], that dictate various seismic design requirements in building codes. Fig. 3.12 shows the NEHRP site classes [11, 12] inferred from the V_{s30} surface of Fig. 3.8 (without regard for the special conditions for site class F). The Christchurch sites are characterized as either NEHRP site class D (blue markers) or class E (red markers). The class E sites primarily correspond to known areas of silty, clayey, or swampy soils such as Papanui and Sydenham. There are also a few sporadic zones of class E soils along the path of the Avon river through the eastern suburbs of the city. Because only those CPT sites that penetrated to a useful depth were used, and because sites in the loess deposits were omitted, the results of Fig. 3.12 do not depict stiff sites in the Port Hills which would be characterized as NEHRP site classes B or C.

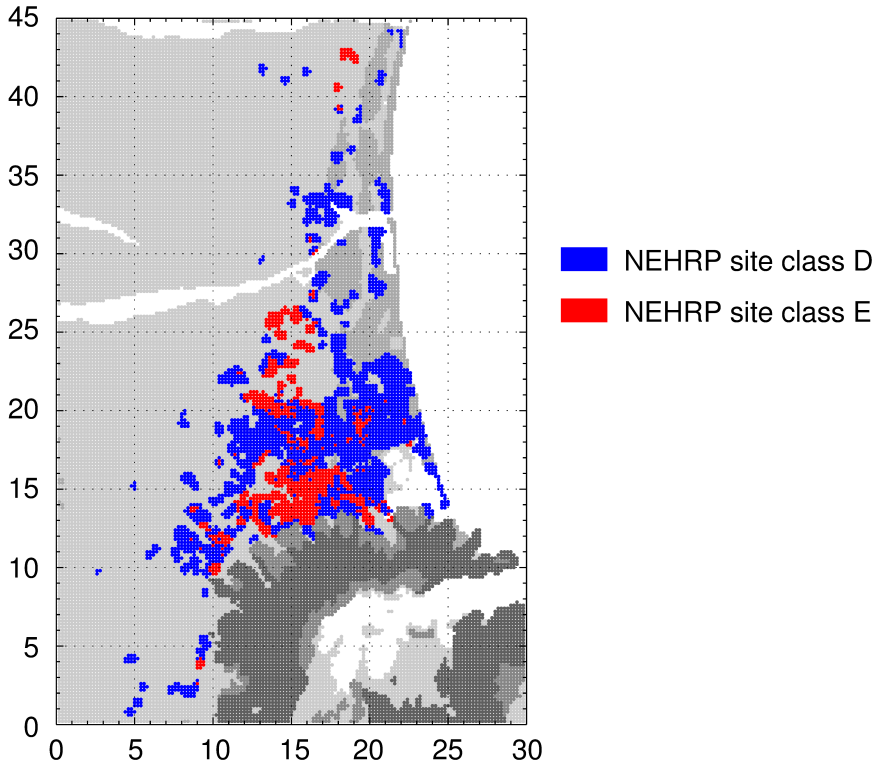

Fig. 3.12: NEHRP site classes for Christchurch V_{s30} surface. Red markers indicate site class E ($V_{s30} \leq 180$ m/s) and blue markers indicate site class D ($180 < V_{s30} \leq 360$ m/s). Criteria for site class F are ignored.

3.6 Liquefaction Severity Identification from V_{sz} Surfaces

The strong shaking associated with the events of the 2010-2011 Canterbury earthquake sequence triggered extensive liquefaction in the Christchurch area. As shown in the residential liquefaction-induced land damage map in Fig. 3.13(b) [20], which presents observations made following the February 2011 earthquake, the surface manifestations and damage associated with this liquefaction were particularly severe in the suburbs to the east and immediate north of the central business district (CBD) near the present-day route of the Avon river.

While the V_{s30} surface map in Fig. 3.8 provides insights on overall site response, as considered in many simplified equations, the surfaces for the shallower target profile depths can also provide insights into liquefaction response, or liquefaction hazard identification, as these profiles focus on the soils in the range of depths at which liquefaction most commonly occurs. The V_{s5} and V_{s10} surfaces shown in Figs. 3.2 and 3.4 correspond reasonably well with the van Ballegooy et al. [20] liquefaction damage map, with areas where liquefaction occurred typically displaying lower V_{sz} values than areas where liquefaction was not observed (the implication being that lower V_s corresponds to lower relative density). For example, the boundary between the yellow and yellow-green markers ($V_{s5} \lesssim 105$ m/s and $V_{s10} \lesssim 130$ m/s) and the light blue markers ($V_{s5} \gtrsim 115$ m/s and $V_{s10} \gtrsim 140$ m/s) in the eastern suburbs near the Avon river roughly approximates the damage/no damage boundaries shown in Fig. 3.13(b), and clearly delineates the liquefaction-susceptible alluvial soils that follow the path of the Avon river from the marine/dune deposits in which severe liquefaction was more rarely observed.

The very soft locations indicated in Figs. 3.2 and 3.4 ($V_{s5} \lesssim 85$ m/s and $V_{s10} \lesssim 105$ m/s) are, perhaps counter-intuitively, primarily areas where liquefaction did not occur. This is likely due to the nature of the soils in these regions, for example, in the soft zones located in the Papanui/Mairehau area north of the CBD and in the Sydenham area immediately south of the CBD, soils in the upper 5-10 m are comprised primarily of silts, clays, and/or sands with high fines contents. While the predominance of these types of soils at shallow depths results in low values of V_{s5} and V_{s10} (and even V_{s30}), these areas do not correspond to severe liquefaction observations as these types of soils are either less susceptible to liquefaction or not liquefiable. These regions of low V_{s5} and V_{s10} values are highly correlated with locations of in-filled swamps, lagoons, and other wet areas as indicated in the 1856 black maps of Christchurch [36, 37].

Because the regions of lowest V_{s5} and V_{s10} in the full surfaces generally do not correspond to liquefaction-susceptible deposits, it is difficult to make any definitive statements as to what these surfaces can provide in terms of identifying liquefaction hazards beyond what is stated above. To remove the effects of such silty or clayey soils, and isolate the V_{sz} magnitudes corresponding to liquefaction-susceptible deposits, the average soil behaviour type index over the first 5 m below the surface is considered. This average index, I_{c5}, is computed as

$$I_{c5} = \frac{\sum (d_i I_{ci})}{\sum d_i} \tag{3.2}$$

where d_i are the depth increments over which each incremental I_{ci} value applies. In the determination of I_{c5}, the uppermost 1.2 m of soil is ignored, as it is assumed that this crustal soil is not necessarily indicative of the soil types in the zone of interest. Due to the omission of the crustal soil, I_{c5} can be more accurately described as the depth weighted average soil behaviour type index from 1.2-5m below the surface. The name I_{c5} is retained as it signifies the maximum considered depth, however, it should be noted that the definition of this term differs from its shear wave velocity counterpart (V_{s5}) despite the similar notation. Appendix B to this report includes the I_{c5} surface developed using the full dataset using a procedure very similar to that used in the development of the V_{sz} surfaces. Similar surfaces for I_c values averaged over other depth intervals are also presented and briefly discussed in Appendix B.

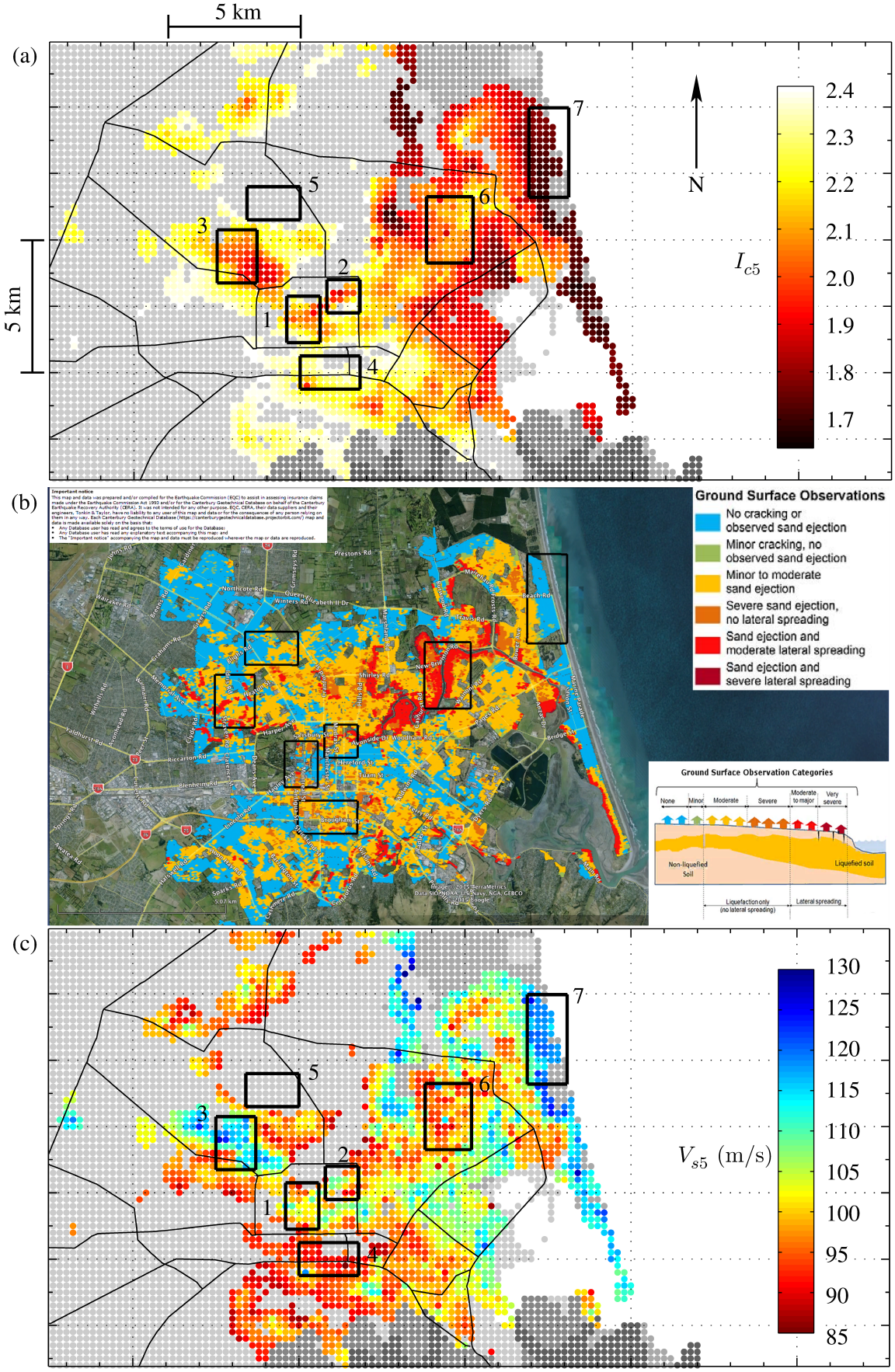

Fig. 3.13: Comparison of I_{c5} and V_{s5} surfaces for areas with $I_{c5} < 2.4$ with observations of liquefaction severity following February 2011 earthquake. (a) $I_{c5} < 2.4$ surface; (b) Liquefaction-induced land damage map after [20]; (c) V_{s5} surface for $I_{c5} < 2.4$. Numbered boxes refer to subregions of Chapter 4.

The I_{c5} surface is used to isolate the V_{s5} values corresponding to the areas of severe liquefaction-related damage by eliminating areas where the shallow soils can be considered less susceptible to liquefaction or not liquefiable using a bounding value of $I_{c5} > 2.4$. While it is conventionally assumed that $I_c > 2.6$ is the value that delimits potentially liquefiable and non-liquefiable deposits, this value is likely conservative in the sense that $I_c = 2.6$ represents a high probability that the soil is not liquefiable rather than a definitive boundary. Additionally, because I_{c5} is an average value across a range of depths, it becomes even more important to consider values lower than 2.6, hence the chosen value of 2.4. Based on a survey of CPT logs with $I_{c5} \approx 2.4$, it was estimated that on average, locations with $I_{c5} \approx 2.4$ have $I_c < 2.6$ over more than 60% of the interval from 1.2-5 m depth. Thus, locations with $I_{c5} > 2.4$ are likely to have soils that are non-liquefiable over more than 40% of this depth interval.

Fig. 3.13(a) shows the I_{c5} surface for only those grid points with $I_{c5} < 2.4$ and Fig. 3.13(c) shows the corresponding V_{s5} surface for the same set of $I_{c5} < 2.4$ grid points. The plot in Fig. 3.13(b) shows the ground surface liquefaction severity observations of van Ballegooy et al. [20] at the same scale and over the same areal extents. The numbered black boxes in these plots correspond to the subregions defined to examine typical profiles as discussed in Chapter 4. A comparison of the V_{s5} surfaces of Figs. 3.2 and 3.13(c) shows that the removal of the grid points with $I_{c5} < 2.4$ resulted in the desired effect of eliminating the lowest V_{s5} values from the surface, at which liquefaction manifestations were generally absent. With the V_{s5} values corresponding to $I_{c5} < 2.4$ removed, it is generally observed that the areas of lower V_{s5} (values less than about 100 m/s) correspond with areas of more severe liquefaction-related phenomena. This is especially true for regions of lower I_{c5} such as those sites along the Avon and Heathcote rivers (northeast and southwest of CBD, respectively). Conversely, areas of higher V_{s5} tend to correspond with areas of less severe or no liquefaction.

Based on Fig. 3.13, it can be seen that while the V_{s5} surface with consideration for $I_{c5} < 2.4$ is clearly not a perfect indicator of liquefaction severity, it appears to work well in an overall sense, especially when considered in tandem with the corresponding I_{c5} surface. Certain areas correspond very well. For example, there is a reasonably high degree of correspondence between V_{s5} magnitude and observations of liquefaction severity along the path of the Avon river (area near subregion 6). In this part of the city, the areas where the surface manifestations of liquefaction were most severe correspond well with $V_{s5} <$ 95-100 m/s, while the areas of minor to moderate liquefaction correspond to higher V_{s5} values. Another interesting V_{s5} transition point is revealed through consideration of the area within subregion 7 in the dune and marine sand deposits near the coast. Within this subregion, there is a clear delineation between V_{s5} values less than about 115 m/s and values greater than about 120 m/s that corresponds nearly exactly with the damage/no damage boundary shown in Fig. 3.13(b). The regions where these general observations tend to fail, such as the large area of low V_{s5} located south of the CBD (vicinity of subregion 4) where there is generally poor correspondence between V_{s5} magnitude and liquefaction severity, also tend to correspond to areas where I_{c5} is relatively high (greater than about 2.2-2.3) despite the low average shear wave velocity. Such locations may be places where the non-I_c-based factors that contribute to the uncertainty in liquefaction potential (e.g., soil age, plasticity, grain size distribution, fabric) reduce the liquefaction potential despite an I_{c5} value that may be classified as potentially liquefiable if considered alone.

Chapter 4

Typical Velocity Profiles for Subregions of Christchurch

The V_{sz} maps developed and discussed in the previous chapter reveal the spatial variation in average shear wave velocity (and implied variation in average shear modulus) inherent to the Christchurch region. These maps are useful for generalized evaluations of the relative stiffness of different areas, however, by comparing the V_{sz} values computed for different target depths, it was shown that there is also a large degree of depth variation in the considered soils. The observed lack of correlation between the average shear wave velocities in the first 5-10 m to those averaged over 30 m profiles suggests that expected seismic site response cannot be well represented by a single metric such as V_{s30}. To investigate this further, typical V_s and soil behaviour type index (I_c) profiles are defined for a series of subregions of the Christchurch area and discussed in this chapter. These typical profiles are used to compare the different stratigraphy that exists in the overall region and assess the typical low-amplitude seismic response of the considered subregions through a comparison of their transfer functions.

4.1 Considered Subregions

Eight subregions were selected from across the greater Christchurch area for the purpose of defining typical velocity profiles. These subregions are indicated by numbered black boxes in the V_{s30} maps of Figs. 3.7 and 3.8, and are assigned the following names and numbers:

1. Central CBD	2. Northeast CBD
3. Fendalton	4. Sydenham
5. Papanui	6. Avondale
7. North New Brighton	8. Kaiapoi

These subregions encompass areas of nearly constant V_{s30} (or areas of particular interest) and were selected to be representative of a variety of site conditions (e.g., soft, stiff, and intermediate soils), surficial soil types (e.g., alluvium, marine/dune), and/or seismic response types (e.g., liquefaction, no liquefaction). Regions 4, 5, and 6 were defined to encompass three areas of relatively low V_{s30} in the fitted surface of Fig. 3.8 where differing soil types are encountered: silty soils in region 4, reclaimed swamp in region 5, and primarily sandy soils in region 6. Regions 3, 7, and 8 consider areas of relatively higher V_{s30}, and represent two general conditions: the relatively shallow gravels of regions 3 and 8, and the dune sands of region 7. Regions 1 and 2 are located in the Christchurch central business district (CBD) and encompass areas of intermediate V_{s30}. Regions 2 and 6 contain portions of the Avon river where many of the areas most severely damaged by liquefaction due to the February 2011 earthquake are located (see Fig. 3.13). The overall degree of liquefaction-induced damage is less in the remaining subregions, though surficial observations of liquefaction were observed in all.

4.2 Typical Profiles for Subregions

Figs. 4.1 through 4.8 show the V_s and I_c profiles for all of the CPT records in each subregion (gray lines) along with characterizations of the mean profiles and the variance in the dataset. The mean V_s and I_c profiles are noted as solid blue lines in each plot, and the dashed lines

represent ± one standard deviation from the mean profiles. For each subregion, the mean profiles were computed using the arithmetic mean considering only the CPT logs with data at each depth, and the standard deviations were obtained by assuming normal distributions in the CPT data at each depth. The number of CPT records with data at each depth, $N(z)$, is indicated for each subregion for reference. To provide a general characterization of each typical velocity profile that is useful for comparisons between the subregions, the V_s plots for each case also note the time-averaged shear wave velocities, V_{sz}, computed for the mean profiles using Eq. (3.1) on 5 m intervals for target profile depths, $z < z_{\text{term}}$ (i.e. the deepest CPT termination depth in the subregion).

As shown in Figs. 4.1-4.8, the uncertainty in the mean V_s profiles is relatively small, with a maximum standard deviation of approximately 50-60 m/s. The uncertainty in the I_c profiles is somewhat greater for most of the subregions, however, the zone of soil behaviour type index bounded by the ± standard deviation profiles appear to be reasonably representative of the CPT-based data, particularly for depths below 5 m. It is also evident that there is much less uncertainty for I_c values less than about 1.8-2.0 (see Figs. 4.2, 4.6, and 4.7) than there is for siltier soils (higher I_c) or near-surface locations. Overall, the relatively small levels of uncertainty observed for these typical V_s and I_c profiles indicates that they provide reasonable representations of the soil profiles in the considered subregions that can be used to evaluate characteristic seismic responses and develop simplified profiles.

Figs. 4.1-4.8 also provide simplified soil behaviour type index profiles developed for each of the 8 subregions. These simplified I_c profiles are useful approximations for the typical soil profiles encountered in each of the considered subregions that could be used to inform constitutive parameters, or as a rough guideline for layering schemes for site-specific numerical analyses. The simplified profiles are based on the mean I_c profiles obtained from the CPT records within each subregion, and provide a granular representation of the soils above the Riccarton Gravel in addition to information on where the top of the Riccarton Gravel is encountered across each subregion (i.e., in Figs. 4.1-4.8 *first* indicates the shallowest depth and *all* indicates the deepest). The layers of the simplified profiles are indicated on the I_c plots in Figs. 4.1-4.8 using solid black lines. An unlabeled transition zone exists between most of the layers, as the depths of the layer boundaries vary within the subregions. Dashed lines in the I_c plots indicate transitions within the layers where there is a distinct change in variance (e.g., at 9.5 m depth in region 1) or small/minor change in the mean profile (e.g., at 23-24 m depth in region 4). Eight borelog records from random locations within each subregion were used to assess the correspondence between the I_c profiles (both the CPT-based and simplified versions) and the actual soil types encountered in each subregion. The soil profiles indicated by these borelogs are provided in Appendix A. Based on the considered borelogs, the I_c profiles obtained from the CPT records appear to reasonably approximate the range of soil profiles and soil types within each subregion.

All of the eight subregions display an approximately 1-2 m deep zone of *crust* soil with lower V_s values and the general behaviour type of a silty sand. As previously discussed, this immediately near-surface zone is not well characterized by the CPT dataset, however, the presence of this crust corresponds with borelog observations (see Appendix A). Another characteristic that is shared by most of the typical profiles is the presence of an approximately 5 m thick layer of higher I_c soils directly above the Riccarton Gravel interface. This zone of siltier soil is present in subregions 1, 2, 4, 5, and 6, and also corresponds to the borehole records. For the purposes of discussion, the considered subregions are grouped according to geographical and geological criteria. These groupings are defined as: Fendalton (region 3); Kaiapoi (region 8); eastern Christchurch (regions 6 and 7); and central Christchurch (regions 1, 2, 4, and 5). The relative similarities and differences for the subregions in each of these groups are discussed in the following sections.

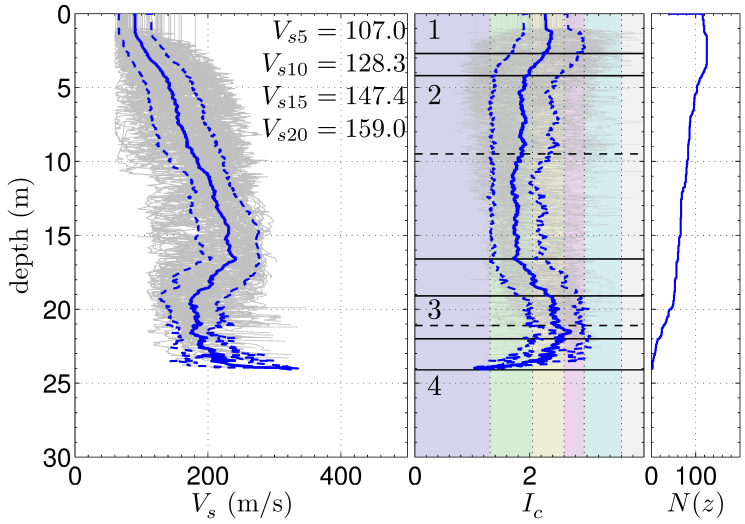

Simplified I_c profile:
Layer 1: 0 to 2.5-4 m
I_c = 2.3, silty sands
Layer 2: 2.5-4 to 17-19 m
I_c = 1.8, sands
Layer 3: 17-19 to 22-24 m
I_c = 2.4, sandy silts
Layer 4: Riccarton Gravel
first: 19.5 m
all: 24 m

Fig. 4.1: V_s and I_c profiles for CPT sites in region 1 (central CBD) for depths above estimated Riccarton gravel surface at each CPT site. $N(z)$ indicates number of CPT records with depth.

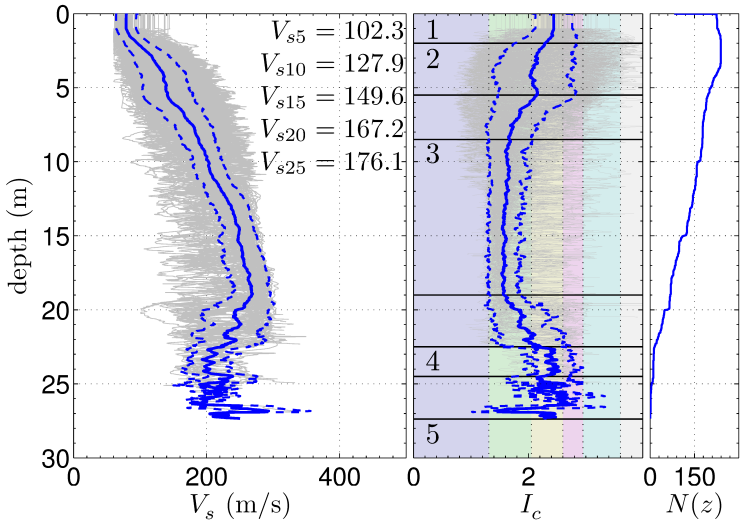

Simplified I_c profile:
Layer 1: 0 to 2 m
I_c = 2.4, sandy silts
Layer 2: 2 to 5.5-7.5 m
I_c = 2.1, silty sands
Layer 3: 5.5-7.5 to 19-22.5 m
I_c = 1.6, sands
Layer 4: 19-22.5 to 24.5-27.3 m
I_c = 2.4, sandy silts
Layer 5: Riccarton Gravel
first: 21.5 m
all: 27.3 m

Fig. 4.2: V_s and I_c profiles for CPT sites in region 2 (northeast CBD) for depths above estimated Riccarton gravel surface at each CPT site. $N(z)$ indicates number of CPT records with depth.

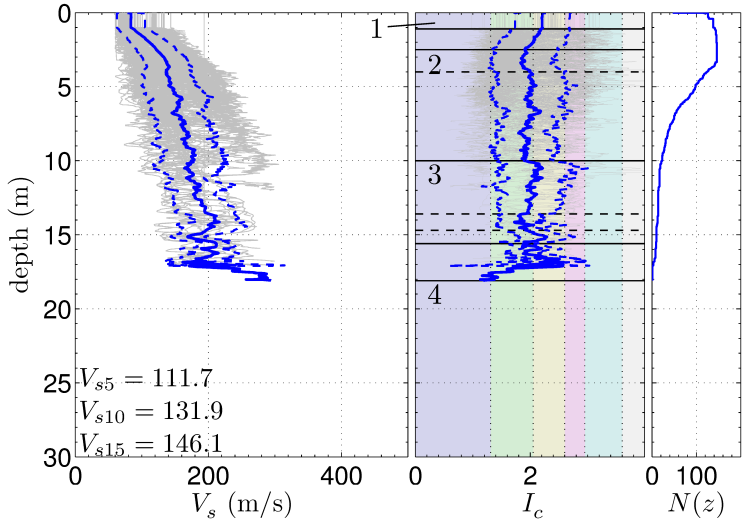

Simplified I_c profile:
Layer 1: 0 to 1.1-2.5 m
I_c = 2.2, silty sands
Layer 2: 1.1-2.5 to 10 m
I_c = 2.0, silty sands
Layer 3: 10 to 15.6-18.1 m
I_c = 2.1, silty sands
Layer 4: Riccarton Gravel
first: 10.5 m
all: 18.1 m

Fig. 4.3: V_s and I_c profiles for CPT sites in region 3 (Fendalton) for depths above estimated Riccarton gravel surface at each CPT site. $N(z)$ indicates number of CPT records with depth.

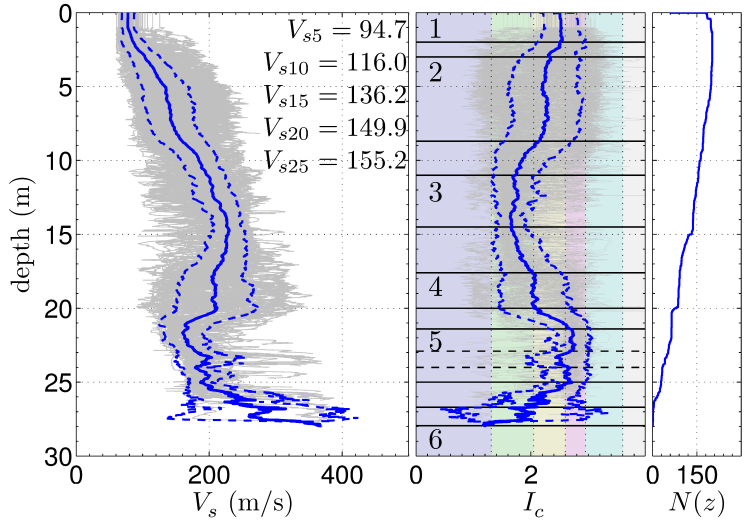

Simplified I_c profile:

Layer 1: 0 to 2-3 m
I_c = 2.5, sandy silts

Layer 2: 2-3 to 8.6-11 m
I_c = 2.3, silty sands

Layer 3: 8.6-11 to 14.5-17.7 m
I_c = 1.7, sands

Layer 4: 14.5-17.7 to 20-21.4 m
I_c = 2.0, silty sands

Layer 5: 20-21.4 m to 25-28 m
I_c = 2.65, clayey silts

Layer 6: Riccarton Gravel
first: 20.5 m
all: 28 m

Fig. 4.4: V_s and I_c profiles for CPT sites in region 4 (Sydenham) for depths above estimated Riccarton gravel surface at each CPT site. $N(z)$ indicates number of CPT records with depth.

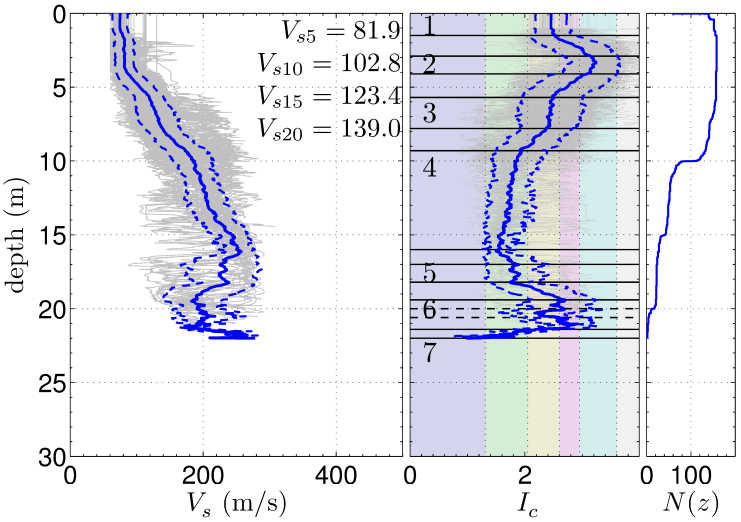

Simplified I_c profile:

Layer 1: 0 to 1.5-2.9 m
I_c = 2.5, sandy silts

Layer 2: 1.5-2.9 to 4.1-5.6 m
I_c = 3.2, clayey silts and peat

Layer 3: 4.1-5.6 to 7.8-9.2 m
I_c = 2.5, sandy silts

Layer 4: 7.8-9.2 to 16-17 m
I_c = 1.5-1.9, sands

Layer 5: 16-17 to 18.1-19.5 m
I_c = 1.8, sands

Layer 6: 18.1-19.5 to 21.5-22 m
I_c = 2.65, clayey silts

Layer 7: Riccarton Gravel
first: 15.5 m
all: 22 m

Fig. 4.5: V_s and I_c profiles for CPT sites in region 5 (Papanui) for depths above estimated Riccarton gravel surface at each CPT site. $N(z)$ indicates number of CPT records with depth.

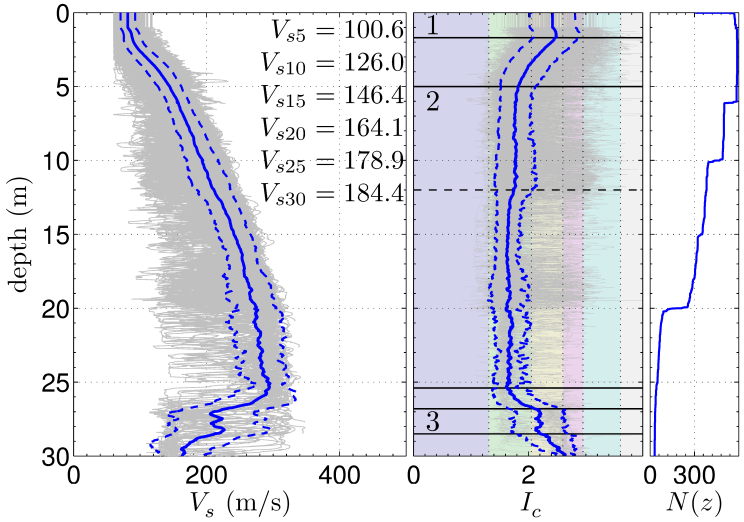

Simplified I_c profile:

Layer 1: 0 to 1.8-5 m
I_c = 2.4, sandy silts

Layer 2: 1.8-5 to 25.2-26.9 m
I_c = 1.7, sands

Layer 3: 25.2-26.9 to 28.5-32 m
I_c = 2.2, silty sands

Layer 4: Riccarton Gravel
first: 26.5 m
all: 32 m

Fig. 4.6: V_s and I_c profiles for CPT sites in region 6 (Avondale) for depths above estimated Riccarton gravel surface at each CPT site. $N(z)$ indicates number of CPT records with depth.

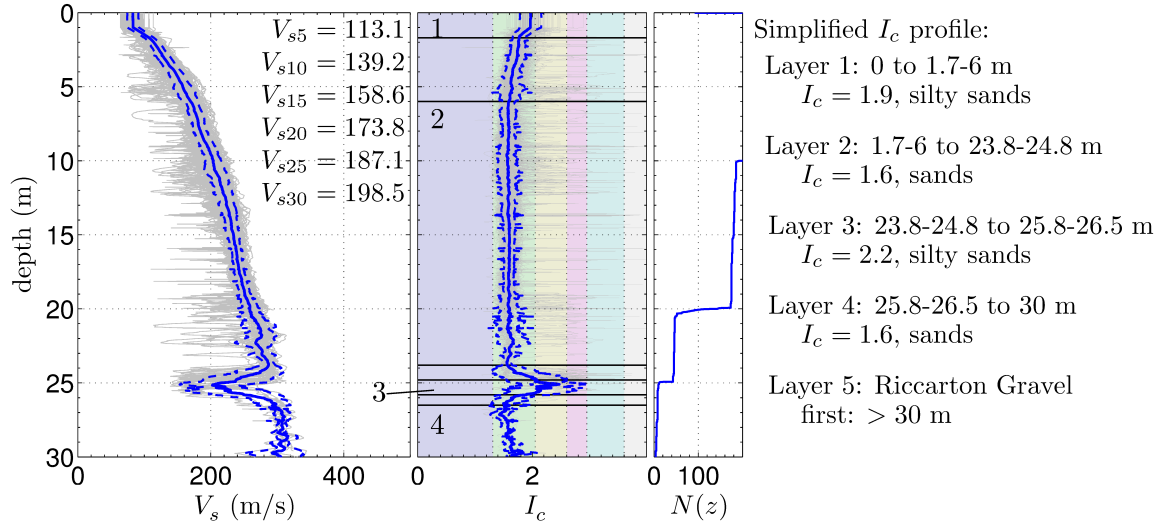

Fig. 4.7: V_s and I_c profiles for CPT sites in region 7 (North New Brighton) for depths above estimated Riccarton gravel surface at each CPT site. $N(z)$ indicates number of CPT records with depth.

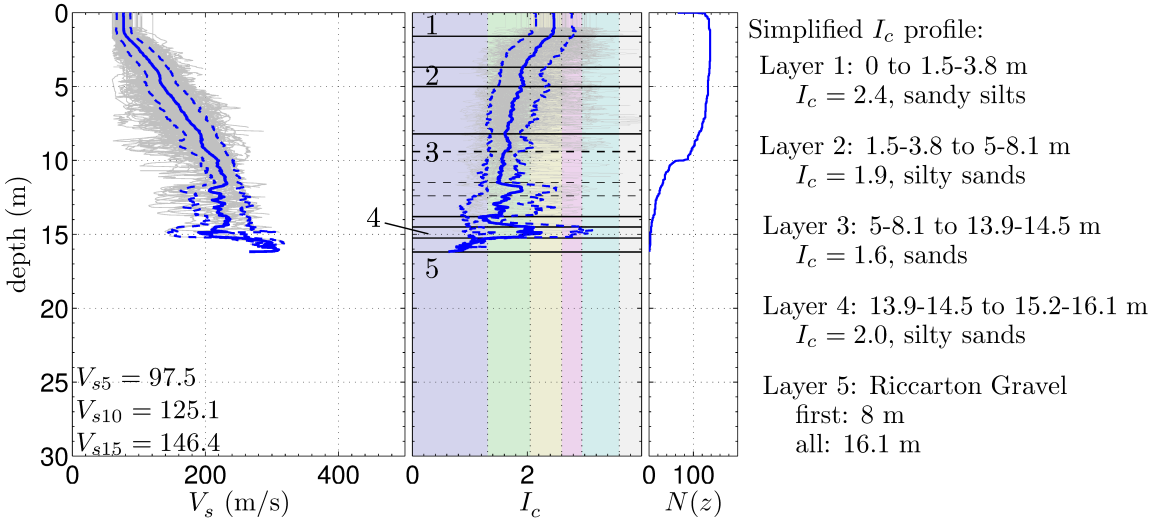

Fig. 4.8: V_s and I_c profiles for CPT sites in region 8 (Kaiapoi) for depths above estimated Riccarton gravel surface at each CPT site. $N(z)$ indicates number of CPT records with depth.

4.2.1 Fendalton Subregion

The Fendalton subregion (region 3) is characterized by a relatively shallow depth to the Riccarton Gravel interface, especially in comparison to most of the other subregions. Additionally, the number of CPT sites in the Fendalton subregion decreases significantly from approximately 3.5 m depth, suggesting that gravels are dominant within the stratigraphy of this subregion. Sites in the Fendalton subregion encounter the Riccarton Gravel surface between about 10.5-18 m depth, thus, the gravels implied by the steady termination of CPT records from 3.5-10.5 m are likely part of the Springston Formation. The Fendalton subregion is located primarily within a region dominated by an over-bank gravel lobe of the Springston Formation [18, (Figs. 15 and 49)], and these observations, combined with the relative lack of CPT records compared to the other subregions, correspond well with the expected local geology. It is a limitation of the current approach that the typical V_s profiles are based only on CPT-penetrable soils. As a result, it is likely that the true in-situ V_s profile and V_{sz} values are underrepresented in the Fendalton subregion, however, the typical profiles still hold for the non-gravel soils.

4.2.2 Kaiapoi Subregion

Region 8 in Kaiapoi is also characterized by a relatively shallow depth to the upper surface of the Riccarton Gravel, with sites encountering the Riccarton Gravel approximately 8-16 m below the ground surface. Significant evidence of liquefaction and lateral spreading was observed for the soils in Kaiapoi, especially after the September 2010 Darfield earthquake [7, 9]. The sands in layers 2 and 3 of the simplified I_c profile have the lower V_s values (and lower I_c values) characteristic of liquefaction-susceptible deposits, especially given the depths at which these materials are located, and are likely representative of the types of materials in which liquefaction occurred. The variation in the number of CPT records with depth shown by the $N(z)$ plot in Fig. 4.8 suggests that Springston Formation gravels may be present above the Riccarton surface from about 5 m depth, but since the decrease in $N(z)$ is gradual from 5-8 m, it is likely that such gravels are not dominant within the subregion. The distinct jump in $N(z)$ at exactly 10 m for region 8 is almost certainly due to testing protocols (i.e. CPT target depth was reached) rather than a feature of the subsurface stratigraphy.

4.2.3 Central Christchurch Subregions

Subregions 1, 2, 4, and 5 are located in the area of Christchurch where the surficial Springston Formation soils are underlain by a wedge of the Christchurch Formation that extends inland to about the western edge of Hagley Park [29, (Fig. 1)]. The likely transitions between these two geologic formations are apparent in the typical profiles for the central and northeast CBD subregions. All of these subregions display a reduction in V_s and increase in I_c immediately above the Riccarton Gravel that is characteristic of the silts, clays, and peats often found at the base of the Christchurch Formation [38], and indicated in the borelogs of Appendix A.

The typical profiles for the two CBD subregions (regions 1 and 2) are similar in form overall. The Riccarton Gravel is deeper beneath region 2 (Riccarton Gravel becomes deeper from west to east, see Fig. 2.4) and the typical profiles in this region are correspondingly deeper than in region 1, but both share the same general features. Silty soils immediately below the surface transition into relatively clean sands, then silty soils return to the profile directly above the Riccarton Gravel interface. For region 1, located in the central CBD, the Springston-Christchurch Formation transition is likely located near 9.5 m depth, where the typical I_c profile moves further into the clean sand range and the variance in I_c becomes notably less. For region 2, in the northeast corner of the CBD, the transition from silty to clean sands that takes place between about 5.5-7.5 m depth (interface of layers 2 and 3 in the simplified I_c profile) likely corresponds with the transition between the Springston and Christchurch Formation soils. The sands from about 10-17 m in the typical I_c profile for region 1, and from 7-20 m depth for region 2, appear to be similar in nature to the sands found in the eastern subregions (Avondale and North New Brighton) where the Christchurch Formation is the dominant surficial geologic unit.

Sites in region 5, located in the reclaimed swampland near Papanui, are typically comprised of sandy silts, clayey silts, and peats in the upper 10 m. The typical V_s profile for this subregion correspondingly has the lowest average shear wave velocity in this zone ($V_{s10} = 102.8$ m/s) of all the considered subregions. Based on the typical profiles, the transition between the Springston and Christchurch Formations for the Papanui subregion likely occurs around 8-10 m below the ground surface, where there is distinct change towards lower I_c values in the typical soil behaviour type profile. The soils in region 4 near Sydenham are similarly silty immediately below the surface (up to about 8.6-11 m depth), but the typical V_s and I_c values in this zone are somewhat higher and lower, respectively, than in region 5. Sites in the Sydenham subregion typically have only a relatively thin layer of clean sand from approximately 11-15 m. The top of this sand layer likely indicates the transition point between the Springston and Christchurch Formation for the sites in this area. Evidence of liquefaction-induced damage was observed

in both regions 4 and 5 following the February 2011 earthquake, however, the severity of the liquefaction-related damages was much less than in some of the other subregions. As shown in Fig. 3.13, there is about a 50/50 split between areas with no observations and areas of minor to moderate sand ejection in region 5, while region 4 contains a mix of areas without observed liquefaction evidence and areas of minor to severe sand ejection (as well as a small zone of moderate lateral spreading). It is likely that the predominantly silty soils (lower liquefaction susceptibility or non-liquefiable) in the upper 10 m are sufficiently thick as to prevent significant liquefaction-related effects from manifesting at the ground surface (or from occurring at all).

4.2.4 Eastern Christchurch Subregions

Regions 6 and 7 are characterized by the greatest depths to the Riccarton Gravel interface of all considered subregions and profiles that are nearly entirely composed of soils with the behaviour type of a relatively clean sand (typical mean $I_c \approx$ 1.6-1.7). In region 6 (Avondale), the top of the Riccarton Gravel is located around 30 m below the surface (slightly shallower for some sites) and there is a distinct zone of silty soils immediately above this interface represented in the typical profiles as a decrease in V_s and increase in I_c. The typical profiles for region 7 (North New Brighton) show the lowest uncertainty of all the considered subregions, consistent with the location of this subregion in the marine/dune sand QMAP unit. None of the CPT logs in this subregion encounter the Riccarton Gravel within the upper 30 m; the Riccarton Gravel surface shown in Fig. 2.4 indicates that this interface is located about 36-38 m below the surface beneath the North New Brighton subregion.

The Avondale subregion includes the present day path of the Avon river, and, as shown in Fig. 3.13, the area encompassed by this subregion corresponds to some of the most widespread observations of severe liquefaction and lateral spreading related damage following the February 2011 earthquake [10, 19, 20]. In contrast, post-earthquake observations in the North New Brighton subregion indicated less severe, and less overall, evidence of liquefaction-related phenomena; and as shown in Fig. 3.13, these observations were constrained to the southwestern corner of the subregion. The typical profiles for these subregions provide some support for these noted differences in liquefaction response. The Avondale profiles in Fig. 4.6 reflect the potential for liquefaction-related phenomena, with generally lower V_s values in the upper 10 m and I_c values indicating behaviour types of predominantly sandy soils, especially below 4-5 m. The profiles for region 7 shown in Fig. 4.7 indicate similar soil types, however, the relative density of these deposits is likely greater (higher V_s and lower I_c) compared to corresponding depths in region 6. Furthermore, because the difference between V_{s5} and V_{s10} for regions 6 and 7 is greater than the differences for the other target depths (with the exception of V_{s30}, which is strongly affected in region 6 by the soft soils immediately above the Riccarton Gravel), it appears that the primary differences in the V_s profiles occur in the immediate near-surface zone. This difference in density at shallow depths, along with the differences in the groundwater table depth for the two subregions (typically at 0-3 m for region 6, and 1-6 m for region 7 per van Ballegooy et al. [31]), provides a potential explanation for the significant differences in liquefaction response within the Avondale and North New Brighton subregions.

4.3 Characterization of Typical Profiles to 30 m Depth

The typical V_s profiles obtained for the considered subregions and shown in Figs. 4.1-4.8 provide a description of the soil shear wave velocities for depths with at least one CPT record. To characterize these profiles up to a depth of 30 m, the estimated Riccarton Gravel surface discussed in Section 2.4 and shown in Fig. 2.4 is used to determine the depth to the Riccarton Gravel at each CPT site, and assumed velocity profiles for the Riccarton Gravel are computed using Eq. (2.2) and appended to the appropriate depths. The 30 m V_s profiles for all 8 subregions are

shown in Fig. 4.9 along with V_{sz} values determined on 5 m intervals from each modified mean V_s profile. As with the previous typical profile plots, the gray lines in Fig. 4.9 show the collected CPT-based V_s values within each subregion, the solid blue lines show the mean profiles, and the dashed lines portray the uncertainty by plotting ± one standard deviation from the mean V_s profile. No uncertainty is considered in the estimated Riccarton Gravel velocity profiles. The fill-in criteria discussed in Section 2.5 is not considered in the computation of these typical 30 m profiles; for a given CPT site within one of the considered subregions, the typical V_s profiles above the Riccarton Gravel are informed only by recorded data.

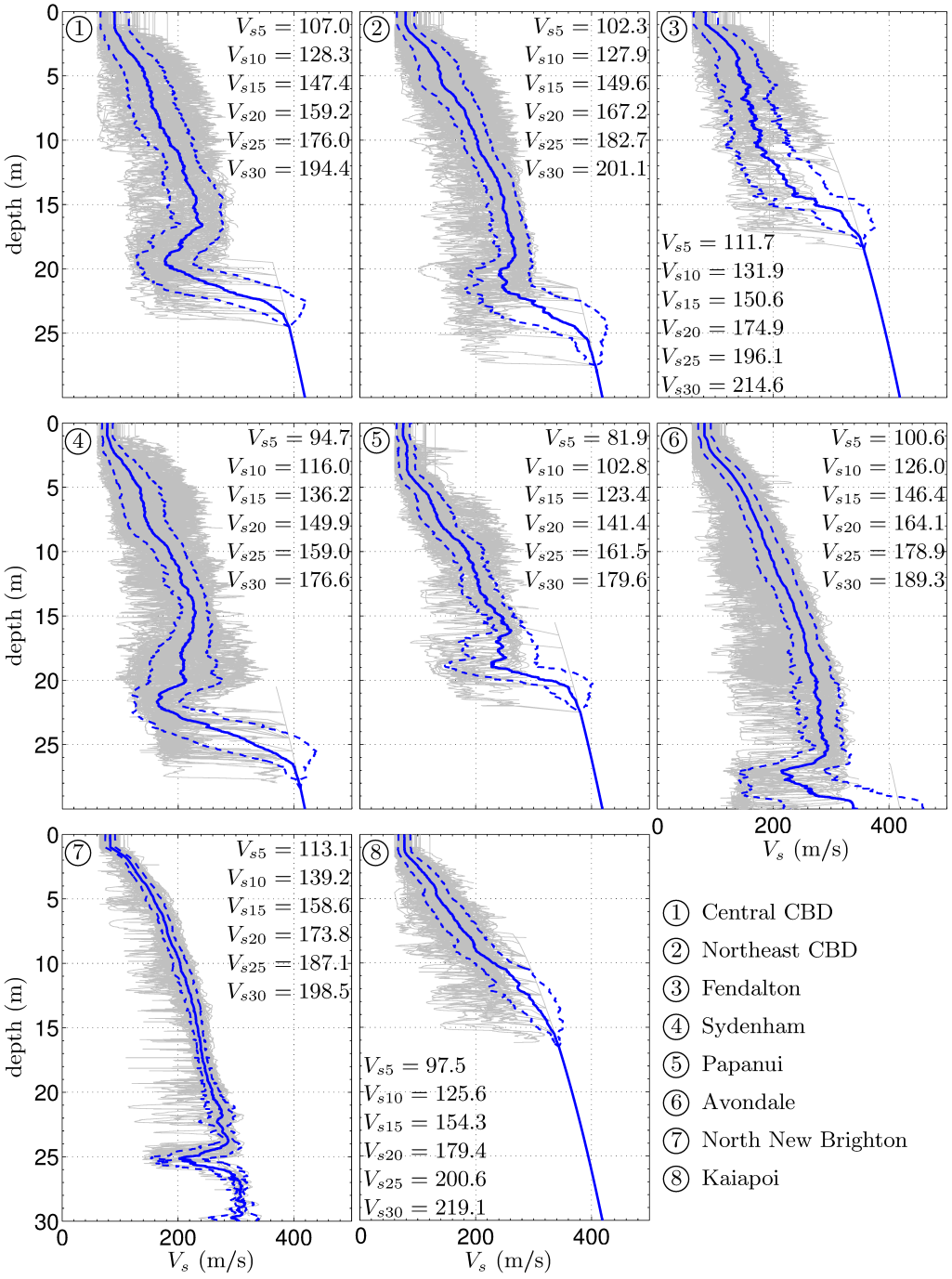

Fig. 4.9: Typical V_s profiles for 8 Christchurch subregions including estimated gravel velocities for depths below top of Riccarton Gravel surface. Region number is noted in upper left of each plot.

In an overall sense, and in the context of the NEHRP site classification system [11, 12] (all of the typical profiles correspond to site class D or E), the V_{s30} values for all of the subregions are nominally the same. However, as shown in Fig. 4.1-4.2, there is a fair amount of variability in the typical V_s profiles for the considered subregions both in terms of the shear wave velocities represented, and in terms of the depth to the top of the Riccarton Gravel. The inclusion of the Riccarton Gravel velocity profiles results in a slight increase in the deepest non-gravel V_{sz} values shown in Figs. 4.1 to 4.8 (e.g., in region 2, $V_{s25} = 176.1$ m/s without gravel velocity and 182.7 m/s with the gravel velocity), as the presence of the Riccarton Gravel at these depths drives up the average shear wave velocity.

4.4 Comparison of Transfer Functions for Typical Profiles

Transfer functions are computed from the mean V_s profiles shown in Fig. 4.9 to investigate the similarities and differences in low-amplitude seismic response for 30 m deep profiles within the considered Christchurch subregions. As shown in Fig. 4.9, several of the subregions with dissimilar V_s profiles are nominally identical in terms of V_{s30} (e.g., regions 4 and 5), and it is of interest to assess to what degree that these differences in soil profile are manifested as differences in surficial site response. Because the transfer functions are based on the assumption of linear response, it is not expected that any observations made here will hold for large amplitude ground motions that induce nonlinear soil behaviour. Factors that are not captured here, such as soil composition, the relative distribution of soil density within the profile, and the location of the groundwater table become more important under large amplitude shaking and will arguably lead to further differences between the seismic response characteristics of the different deposits. However, the transfer functions for these velocity profiles provide a simple means with which to evaluate V_{s30} as a predictive metric for site response in the Christchurch area.

Fig. 4.10 shows the computed transfer functions for each subregion in terms of the variation in amplification factor with frequency. These transfer functions were computed assuming constant density $\rho = 1.8$ Mg/m^3 and constant damping ratio $\xi = 5\%$ throughout all profiles. Regions with similar V_{s30} values are grouped together in Fig. 4.10 to emphasize the relative differences in seismic response indicated for regions that are classified as similar according to V_{s30}-based criteria such as the NEHRP site classes. The upper plot of Fig. 4.10 shows the soft subregions, Sydenham (region 4) and Papanui (region 5) where $V_{s30} < 180$ m/s; the middle plot includes the intermediate V_{s30} subregions, Avondale (region 6), North New Brighton (region 7), and the two CBD regions (regions 1 and 2); and the lower plot shows the two stiff subregions, Fendalton (region 3) and Kaiapoi (region 8) where $V_{s30} > 210$ m/s due primarily to the presence of the previously discussed shallow gravels. As shown in Fig. 4.10, there is quite a bit of difference between the transfer functions computed from the typical 30 m V_s profiles for subregions 1-8. The differences are most apparent in the upper and lower plots of Fig. 4.10, which compare the transfer functions for the softest and stiffest regions, respectively.

The typical profiles for regions 4 and 5 have essentially identical V_{s30} values (176.6 and 179.6 m/s, respectively). However, based on the results of Fig. 4.10, given identical input motions at 30 m depth, the resulting surficial motions, and the associated effects on structural response, would likely be quite different. The peak amplifications occur for different frequencies (max amplification for region 4 at 4.7 Hz and at 2.5 Hz for region 5), and have different amplitudes (max amplification factor is 2.4 in region 4 and 2.8 in region 5). In addition, the peak amplification factor for region 4 occurs in the second mode rather than in the first mode as for region 5, and the amplification for higher modes in region 4 is generally greater than or equal to that in region 5. The typical profiles for regions 3 and 8 are also nominally identical in terms of V_{s30} and show a similar difference in peak amplification magnitude (2.2 in region 3, 2.5 in region 8). The transfer functions for these subregions also show a difference in frequency for the first mode

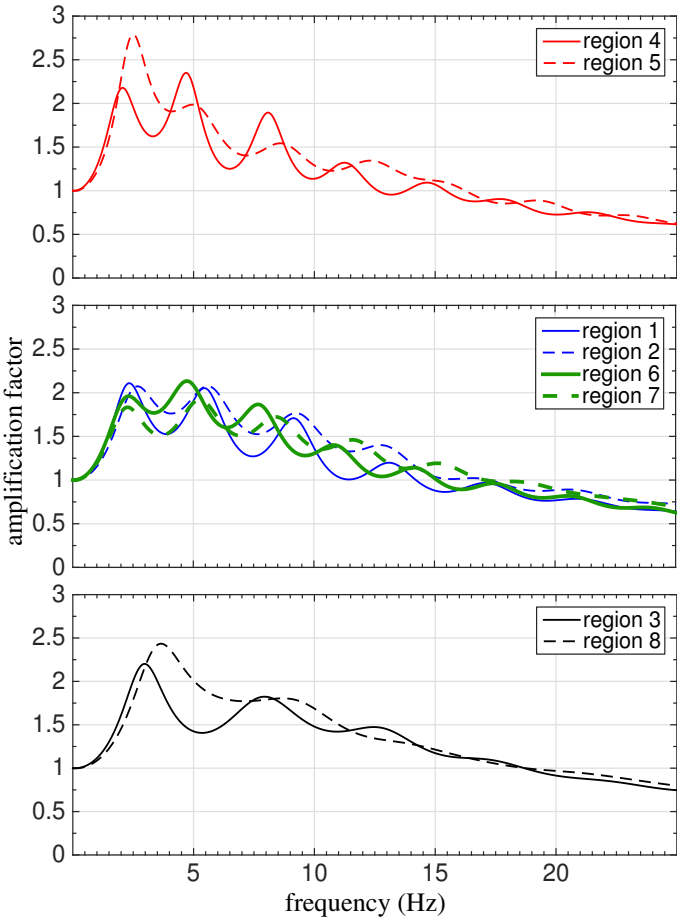

Fig. 4.10: Transfer functions for 8 Christchurch subregions grouped by V_{s30}.

(2.8 Hz in region 3, 3.7 Hz in region 8). The higher modes in Fendalton have amplification factors greater than or equal to those in Kaiapoi and occur at lower frequencies.

The transfer functions for the subregions shown in the middle plot of Fig. 4.10 (regions 1, 2, 6, and 7) are more similar to each other than in the previously discussed groupings, but differences are still apparent. The V_{s30} values for the profiles in all four of these subregions are within about 12 m/s of each other, however, there is a clear distinction between the transfer functions for the CBD (regions 1 and 2) and eastern Christchurch (regions 6 and 7) subregions that does not correspond to their relative V_{s30} values. The magnitude of the peak amplification in the first two modes of regions 1 and 2 are nominally identical at about 2.1, but the modal troughs in region 2 are less pronounced and the modal peaks are generally greater in amplitude beyond the second mode. For the eastern Christchurch subregions, the amplification and frequency for the first mode are similar (amplification of about 1.6-1.9 at 2.25 Hz) and the second mode response has a larger amplification factor in both cases. The higher modes in region 6 generally occur at lower frequencies than in region 7, and beyond the third mode, the amplification factors in the higher modes for region 7 are generally higher.

REFERENCES

[1] McGann C, Bradley B, Taylor M, Wotherspoon L, Cubrinovski M. Applicability of existing empirical shear wave velocity correlations to seismic cone penetration test data in Christchurch New Zealand. Soil Dynamics and Earthquake Engineering 2015;doi:http://dx.doi.org/10.1016/j.soildyn.2015.03.021.

[2] McGann C, Bradley B, Taylor M, Wotherspoon L, Cubrinovski M. Development of an empirical correlation for predicting shear wave velocity of Christchurch soils from cone penetration test data. Soil Dynamics and Earthquake Engineering 2015;doi:http://dx.doi.org/10.1016/j.soildyn.2015.03.023.

[3] Lee R, Bradley B, Pettinga J, Hughes M, Graves R. Ongoing development of a 3D seismic velocity model of Canterbury, New Zealand for broadband ground motion simulation. In: New Zealand Society for Earthquake Engineering Annual Conference. Auckland, March 21-23, Paper No. 8; 2014.

[4] Bradley B, Cubrinovski M. Near-source strong ground motions observed in the 22 February 2011 Christchurch earthquake. Seismological Research Letters 2011;82(6):853–65.

[5] Bradley B. Strong ground motion characteristics observed in the 4 September 2010 Darfield, New Zealand earthquake. Soil Dynamics and Earthquake Engineering 2012;42:32–46.

[6] Bradley B. Ground motions observed in the Darfield and Christchurch earthquakes and the importance of local site response effects. New Zealand Journal of Geology and Geophysics 2012;55(3):279–86.

[7] Cubrinovski M, Bradley B, Wotherspoon L, Green R, Bray J, Wood C, et al. Geotechnical aspects of the 22 February 2011 Christchurch earthquake. Bulletin of the New Zealand Society for Earthquake Engineering 2011;44(4):205–26.

[8] Cubrinovski M, Bray J, Taylor M, Giorgini S, Bradley B, Wotherspoon L, et al. Soil liquefaction effects in the central business district during the February 2011 Christchurch earthquake. Seismological Research Letters 2011;82(6):893–904.

[9] Cubrinovski M, Green R, Allen J, Ashford S, Bowman E, Bradley B, et al. Geotechnical reconnaissance of the 2010 Darfield (Canterbury) earthquake. Bulletin of the New Zealand Society for Earthquake Engineering 2010;43(4):243–320.

[10] GEER. Geotechnical Reconnaissance of the 2010 Darfield (New Zealand) Earthquake. GeoEngineering Extreme Events Reconnaissance (GEER) Association; 2010. R. A. Green and M. Cubrinovski, eds., Report No. GEER-024.

[11] Building Seismic Safety Council . NEHRP Recommended Provisions for Seismic Regulations for New Buildings and Other Structures, Part I: Provisions. Report No. FEMA-450, Federal Emergency Management Agency, Washington, D.C.; 2003.

[12] American Society of Civil Engineers . Minimum Design Loads for Buildings and Other Structures (7-10, third printing). Standards ASCE/SEI 7-10; 2013.

[13] Eurocode 8 . Design of Structures for Earthquake Resistance, Part 1: General Rules, Seismic Actions and Rules for Buildings. EN 1998-1, European Committee of Standardization (CEN); 2004.

[14] Standards New Zealand . Structural Design Actions Part 5: Earthquake Actions – New Zealand. NZS1170.5; 2004.

[15] McVerry G, Zhao J, Abrahamson N, Somerville P. New Zealand acceleration response spectrum attenuation relations for crustal and subduction zone earthquakes. Bulletin of the New Zealand Society for Earthquake Engineering 2006;39(1):1–58.

[16] Bradley B. NZ-Specific Pseudo-Spectral Acceleration Ground Motion Prediction Equations Based on Foreign Models. Research report 2010-03, University of Canterbury, Department of Civil Engineering; 2010.

[17] Abrahamson N, Silva W. Summary of the Abrahamson & Silva NGA ground-motion relations. Earthquake Spectra 2008;24(1):67–97.

[18] Brown L, Weeber J. Geology of the Christchurch urban area. Lower Hutt, New Zealand: Institute of Geological and Nuclear Sciences Ltd.; 1992.

[19] GEER. Geotechnical Reconnaissance of the 2011 Christchurch, New Zealand Earthquake. Geo-Engineering Extreme Events Reconnaissance (GEER) Association; 2011. M. Cubrinovski, R. A. Green, and L. Wotherspoon, eds., Report No. GEER-027.

[20] van Ballegooy S, Malan P, Lacrosse V, Jacka M, Cubrinovski M, Bray J, et al. Assessment of liquefaction-induced land damage for residential Christchurch. Earthquake Spectra 2014;30(1):31–55.

[21] Canterbury Geotechnical Database . `https://canterburygeotechnicaldatabase.projectorbit.com`; 2012.

[22] McGann C, Bradley B, Wotherspoon L, Cox B. Comparison of a Christchurch-specific CPT-V_s correlation and V_s derived from surface wave analysis for strong motion station velocity characterization. Bulletin of the New Zealand Society for Earthquake Engineering 2015;48(2).

[23] Canterbury Earthquake Recovery Authority (CERA) . `http://cera.govt.nz/land-information/land-zones`; 2014.

[24] Robertson P, (Fear) Wride C. Evaluating cyclic liquefaction potential using the cone penetration test. Canadian Geotechnical Journal 1998;35(3):442–59.

[25] Idriss I, Boulanger R. Soil Liquefaction During Earthquakes. Earthquake Engineering Research Institute (EERI), MNO-12; 2008.

[26] Wood C, Cox B, Wotherspoon L, Green R. Dynamic site characterization of Christchurch strong motion stations. Bulletin of the New Zealand Society for Earthquake Engineering 2011;44(4):195–204.

[27] Wotherspoon L, Orense R, Bradley B, Cox B, Wood C, Green R. Geotechnical characterisation of Christchurch strong motion stations. Earthquake Commission Biennial Grant Report, Project No. 12/629; 2013.

[28] Brown L, Beetham R, Paterson B, Weeber J. Geology of Christchurch, New Zealand. Environmental & Engineering Geoscience 1995;1(4):427–88.

[29] Begg J, Jones K, Rattenbury M, Ramilo R. 3D geological and geotechnical models of the Christchurch urban area. In: Proc. 19th New Zealand Geotechnical Society (NZGS) Symposium. Queenstown, New Zealand, November 20-23; 2013.

[30] Forsyth P, Barrell D, Jongens R. Geology of the Christchurch area: scale 1:250,000. Institute of Geological & Nuclear Sciences 1:250,000 geological map 16: Lower Hutt: GNS Science; 2008.

[31] van Ballegooy S, Cox S, Thurlow C, Rutter H, Reynolds T, Harrington G, et al. Median water table elevation in Christchurch and surrounding area after the 4 September 2010 Darfield Earthquake: Version 2. GNS Science Report 2014/18; 2014.

[32] Lin YC, Joh SH, Stokoe K. Analysis of the UTexas 1 surface wave dataset using the SASW methodology. In: Geo-Congress 2014 Technical Papers, GSP 234. 2014, p. 830–9.

[33] Khalaf G, Månnson K, Shuhur G. Modified ridge regression estimators. Communications in Statistics–Theory and Methods 2013;42(8):1476–87.

[34] Boore D. Estimating $\overline{V}_{s30}$ (or NEHRP site classes) from shallow velocity models (depths < 30 m). Bulletin of the Seismological Society of America 2004;94(2):591–7.

[35] Boore D, Thompson E, Cadet H. Regional correlations of V_{s30} and velocities averaged over depths less than and greater than 30 meters. Bulletin of the Seismological Society of America 2011;101(6):3046–59.

[36] Wilson J. Christchurch swamp to city. A short history of the Christchurch Drainage Board 1875-1989. Lincoln: Te Waihora Press; 1989.

[37] Information Services Christchurch City Council . Christchurch area showing waterways swamps & vegetation cover in 1856. `http://resources.ccc.govt.nz/files/blackmap-environmentecology.pdf`; 2006. Accessed: 26 August 2014.

[38] White P. Geological Model of the Christchurch Formation and Springston Formation. GNS Science Consultancy Report 2007/117; 2007.

Appendix A

Sample Borelogs for Christchurch Subregions

Eight borelog records were obtained from the Canterbury Geotechnical Database [21] for random locations within each of the Christchurch subregions discussed in Chapter 4. Summaries of the soil profiles (up to 30 m) indicated by these borelogs are provided in Figs. A.1-A.8. The individual borehole ID numbers from the database are indicated along the top row of each summary, and the simplified soil behaviour type index (I_c) profile for each subregion is noted in the right-most column. As shown, there is generally good agreement between the typical soil behaviour type profiles represented by the simplified profiles and the actual soil types indicated in the borelogs.

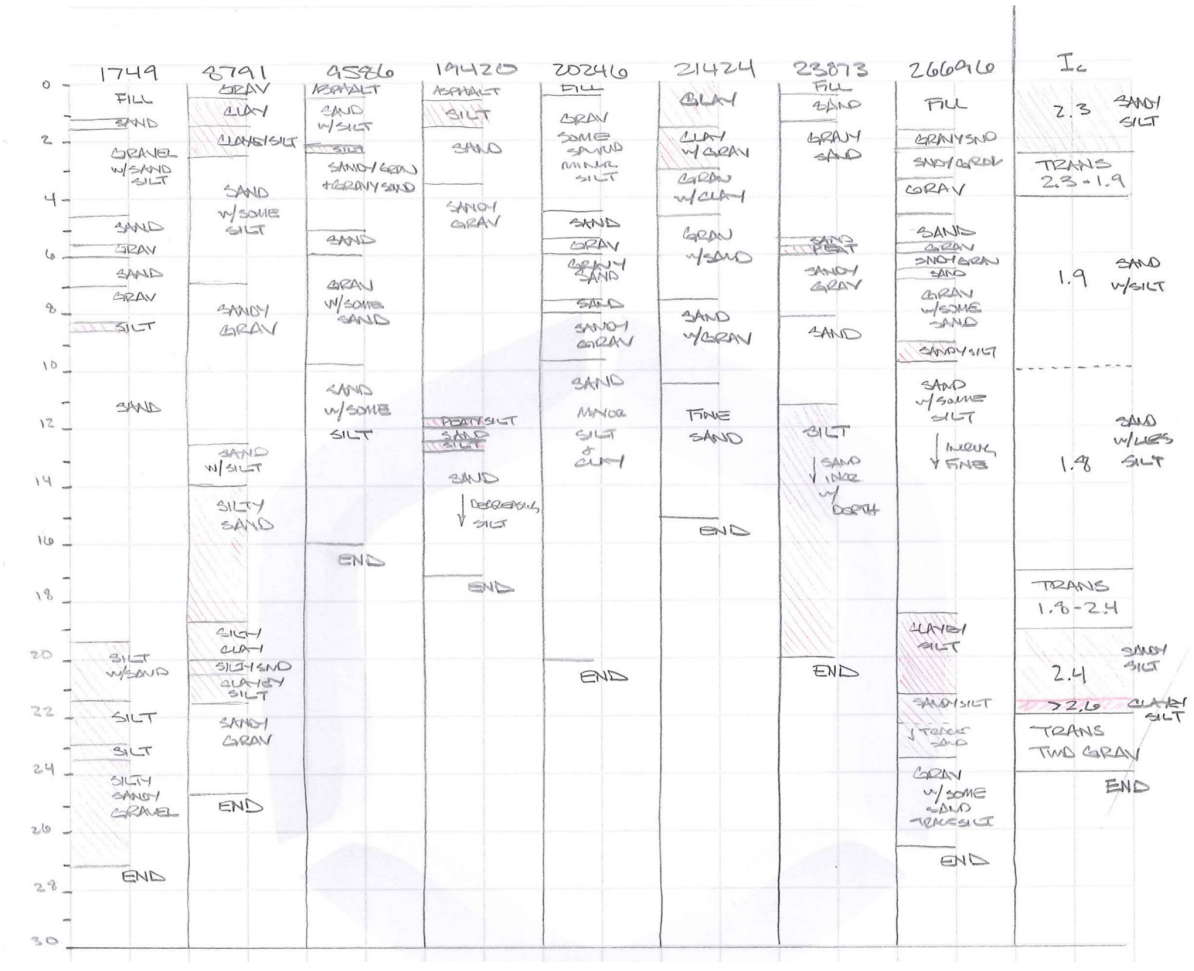

Fig. A.1: Summary of eight sample borelogs from region 1 (Central CBD) alongside simplified I_c profile.

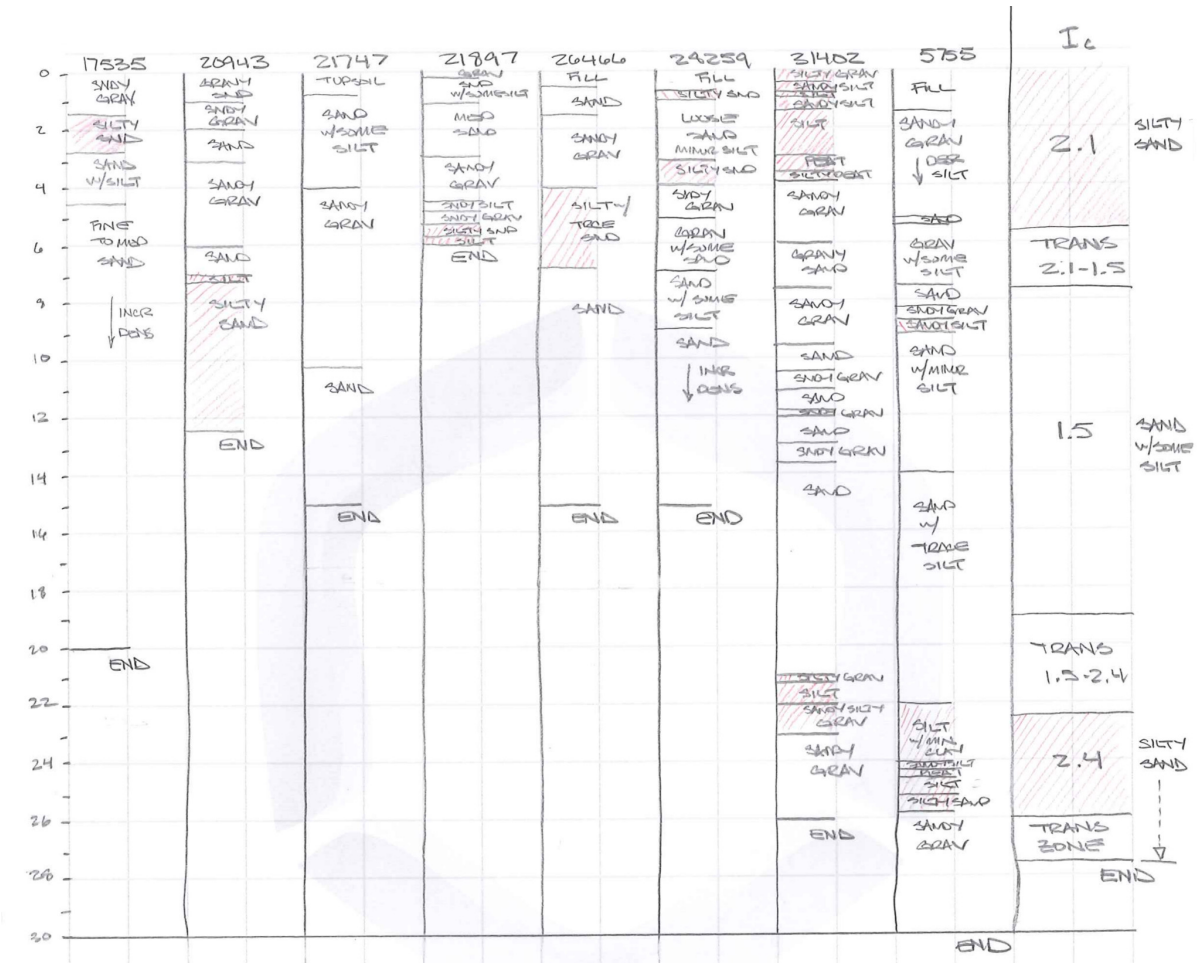

Fig. A.2: Summary of eight sample borelogs from region 2 (Northeast CBD) alongside simplified I_c profile.

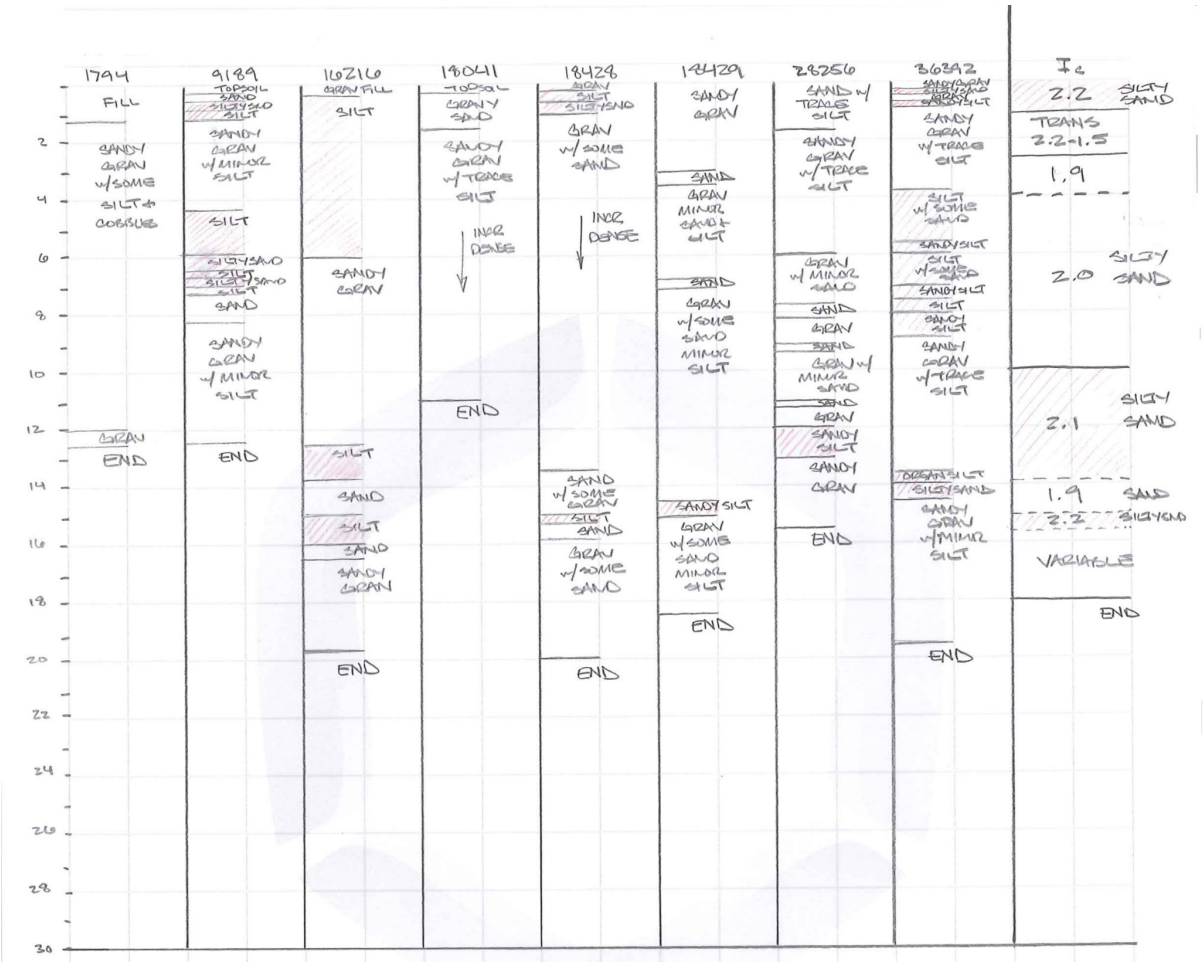

Fig. A.3: Summary of eight sample borelogs from region 3 (Fendalton) alongside simplified I_c profile.

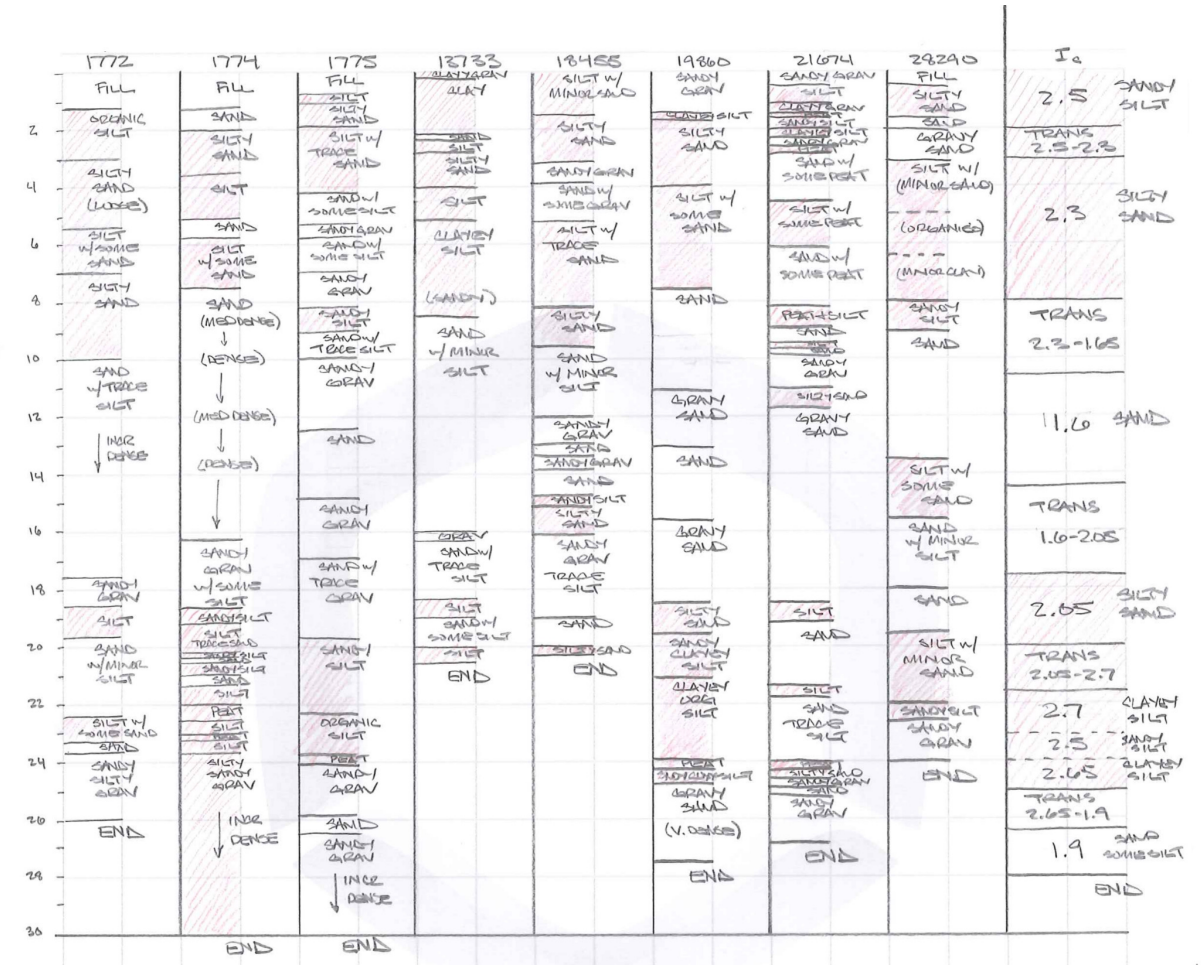

Fig. A.4: Summary of eight sample borelogs from region 4 (Sydenham) alongside simplified I_c profile.

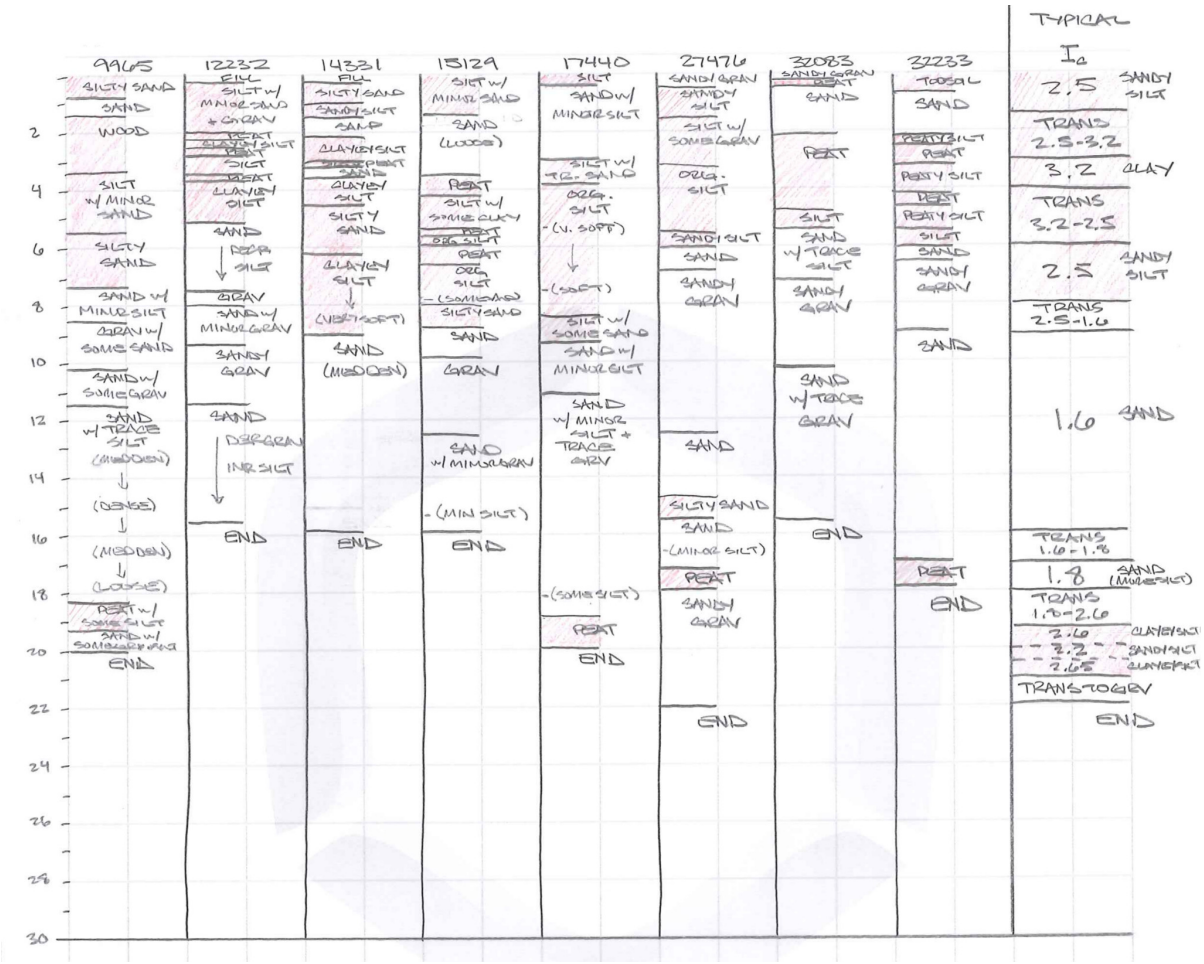

Fig. A.5: Summary of eight sample borelogs from region 5 (Papanui) alongside simplified I_c profile.

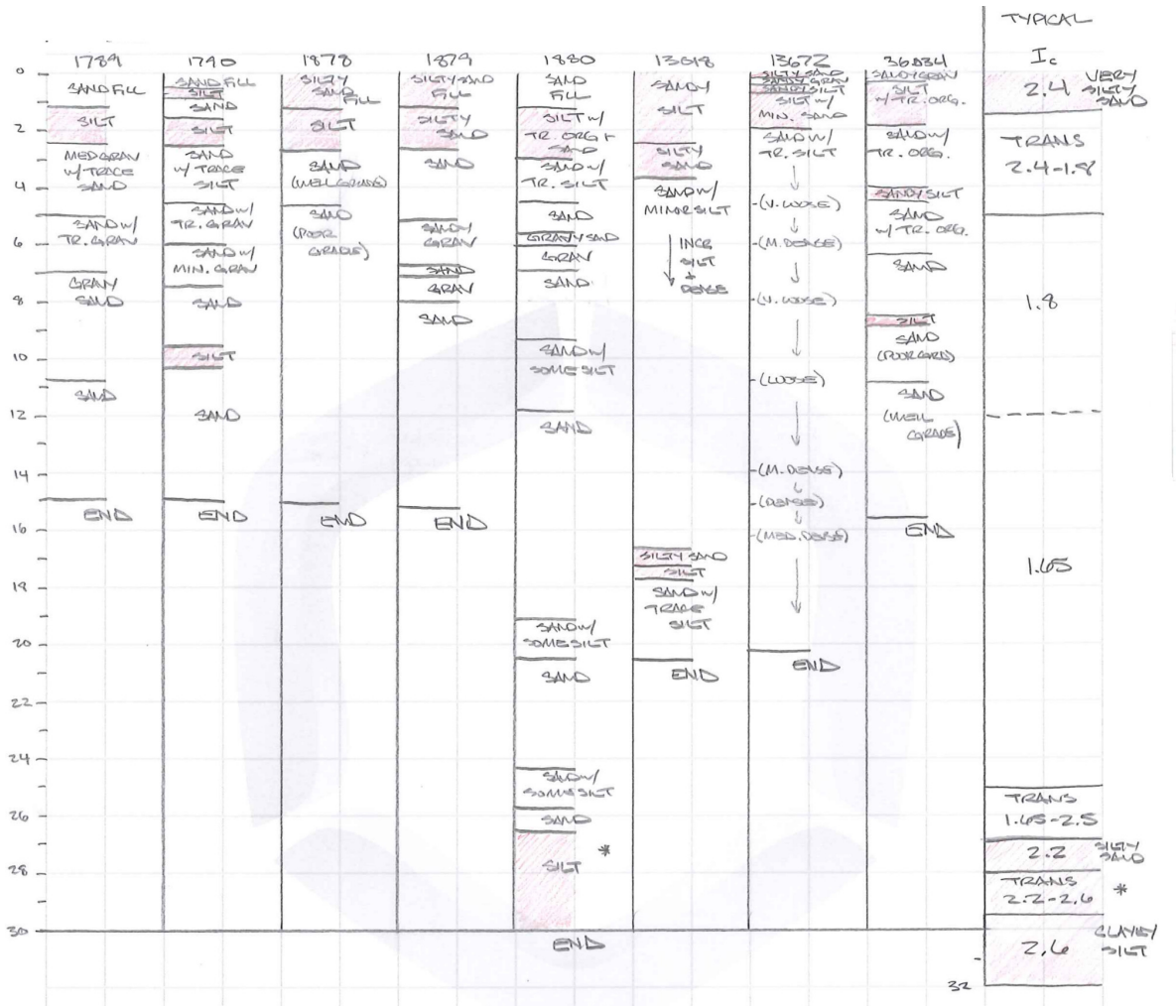

Fig. A.6: Summary of eight sample borelogs from region 6 (Wainoni) alongside simplified I_c profile.

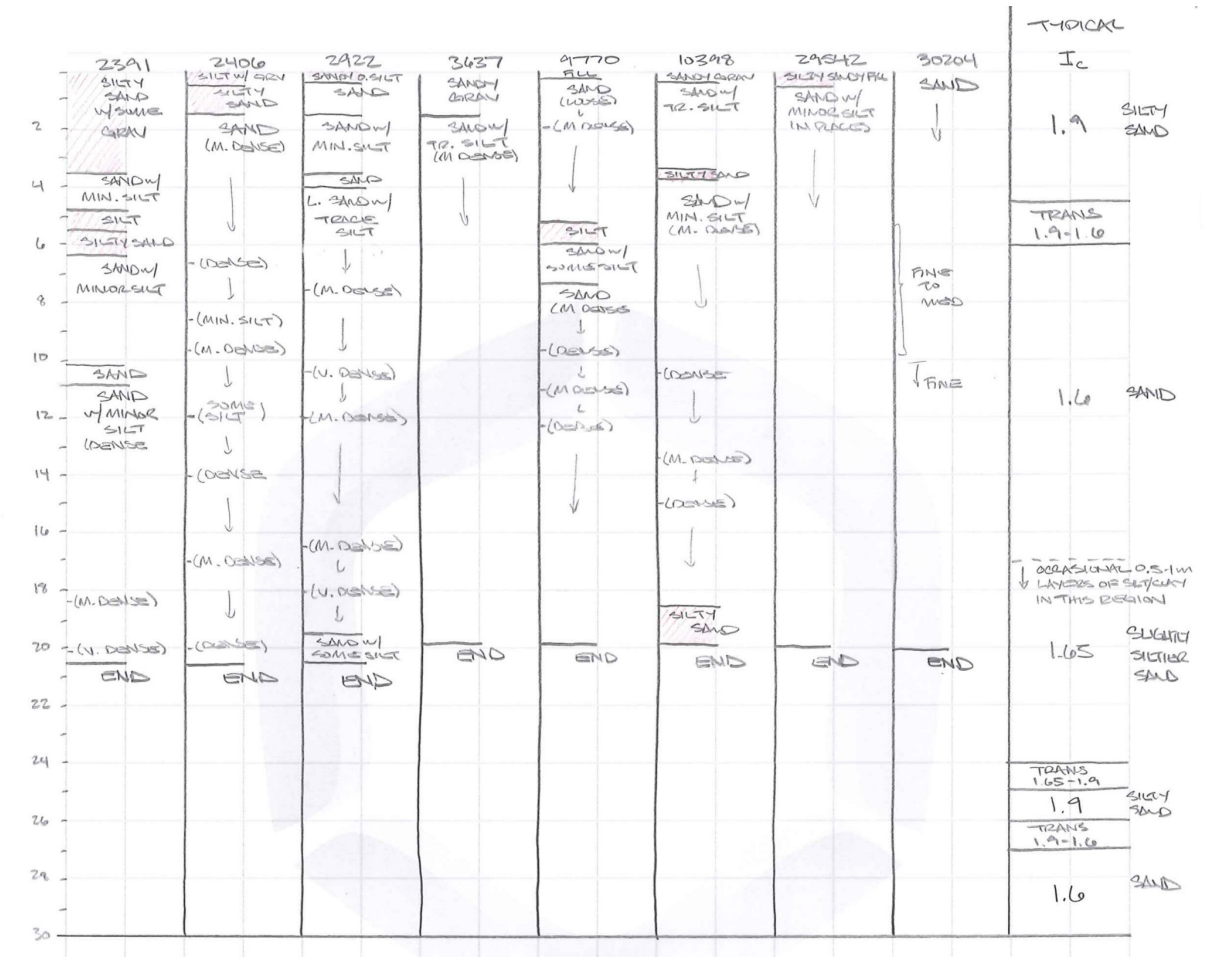

Fig. A.7: Summary of eight sample borelogs from region 7 (North New Brighton) alongside simplified I_c profile.

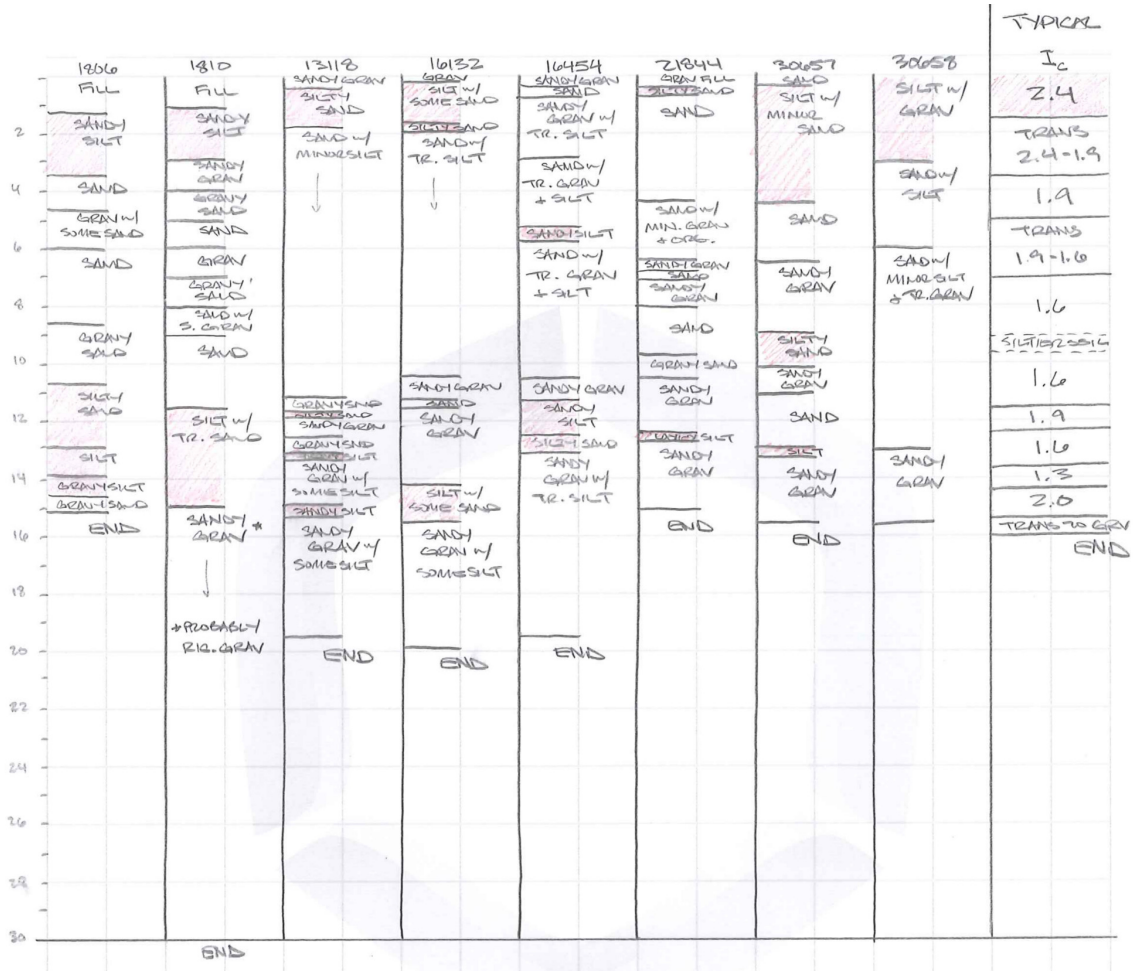

Fig. A.8: Summary of eight sample borelogs from region 8 (Kaiapoi) alongside simplified I_c profile.

Appendix B

Depth-Weighted Average Soil Behaviour Type Index Surfaces

The discussion in Section 3.6 concerning the degree of correlation between V_{s5} and observed liquefaction severity introduced the concept of a depth-weighted average of the soil behaviour type index over the interval from 1.2-5 m below the surface. This average index was given the name I_{c5}, as it represents an average over the non-crustal soils up to 5 m depth, and was used to remove the areas with the lowest V_{s5} values (corresponding to high I_{c5} values and low probability of liquefaction) to aid in idenfifying the range of V_{s5} values that correspond with liquefaction severity observations in liquefiable (or at least potentially liquefiable) soil deposits. Fig. B.1 presents the full I_{c5} surface generated from the processed CPT data set, using similar procedures and covering the same spatial extents as used in the development of the V_{sz} surfaces shown in Chapter 3.

Surfaces corresponding to two additional average indices were also developed. These additional indices consider different depth intervals. Fig. B.2 shows the surface corresponding to I_{c8}, which is computed similarly to I_{c5}, see Eq. (3.2), but over the depth interval of 1.2-8 m below the ground surface. Fig. B.3 shows the surface corresponding to I_{c10}, which is defined as the depth-weighted average over the interval from 5-10 m below the ground surface. Comparison of these surfaces can aid in identifying soil behaviour type trends across the considered area and the range of considered depths. Figs. B.4–B.6 show the same surfaces as Figs. B.1–B.3 but with a modified colormap chosen to highlight the difference between soils that are likely to be liquefiable ($I_{cz} < 2.4$ in this case) and soils that are unlikely to be liquefiable ($I_{cz} > 2.4$). This plotting modification reveals that in an average sense, I_c tends to become less as depth increases up to 10 m for most of the considered area.

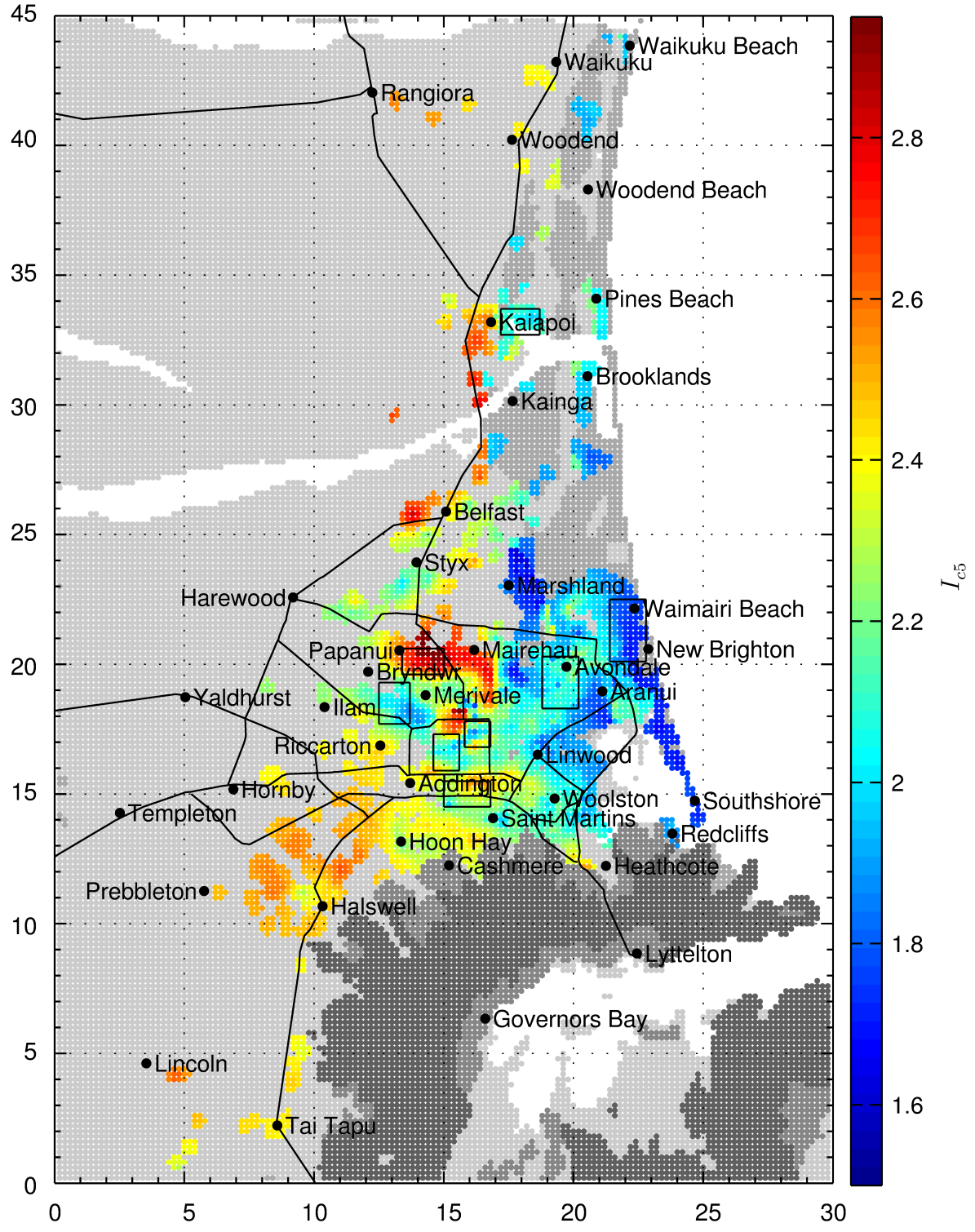

Fig. B.1: I_{c5} surface on uniform 200 × 200 m grid. NZMG projection; horizontal and vertical axes indicate km from lower left corner of map. Latitude/Longitude (WGS84) bounds for the map are (−43.6811°, 172.4418°) and (−43.2773°, 172.8151°). Predictions are only provided in each grid cell if there is one or more CPT record within 300 m.

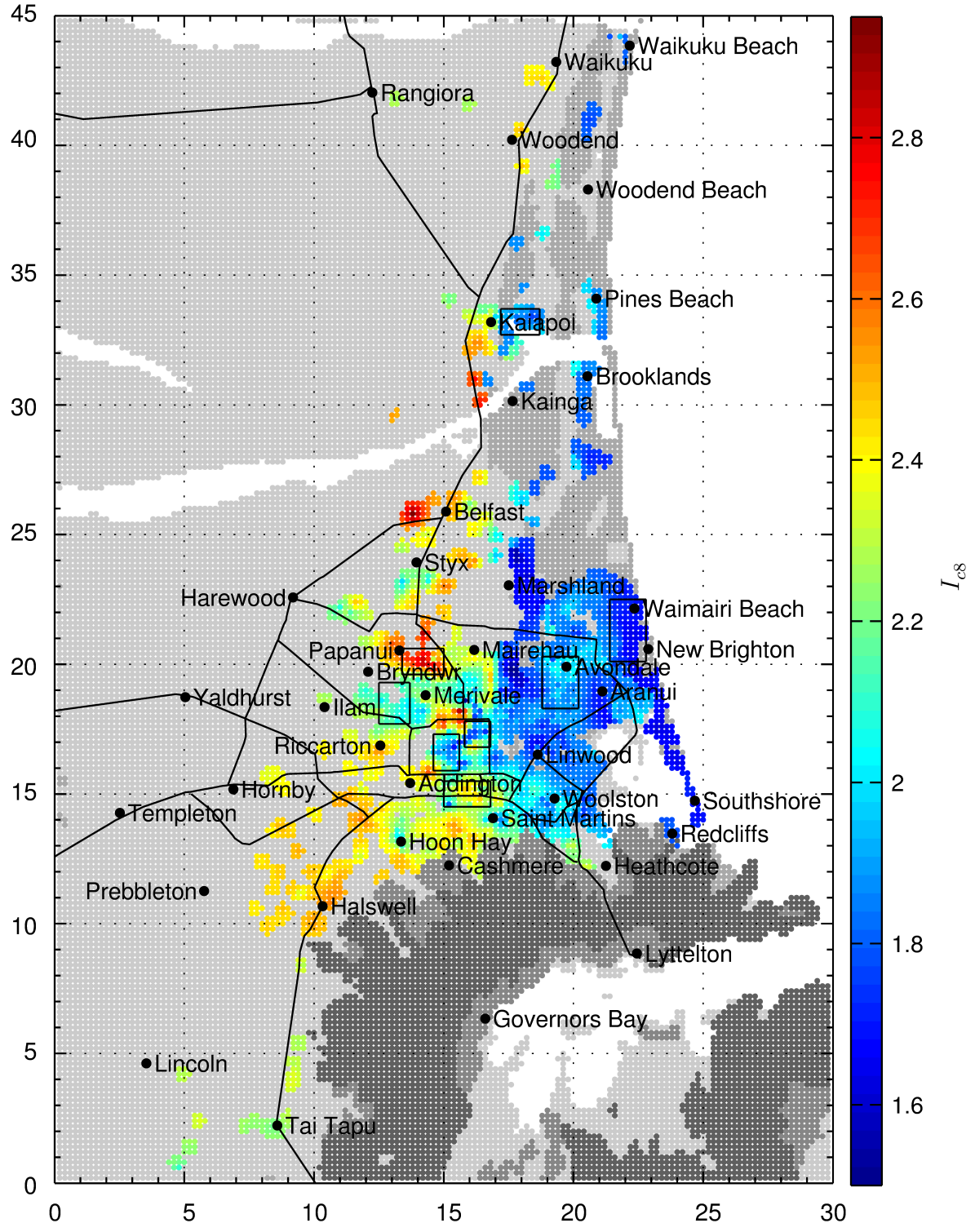

Fig. B.2: I_{c8} surface on uniform 200 × 200 m grid. NZMG projection; horizontal and vertical axes indicate km from lower left corner of map. Latitude/Longitude (WGS84) bounds for the map are (−43.6811°, 172.4418°) and (−43.2773°, 172.8151°). Predictions are only provided in each grid cell if there is one or more CPT record within 300 m.

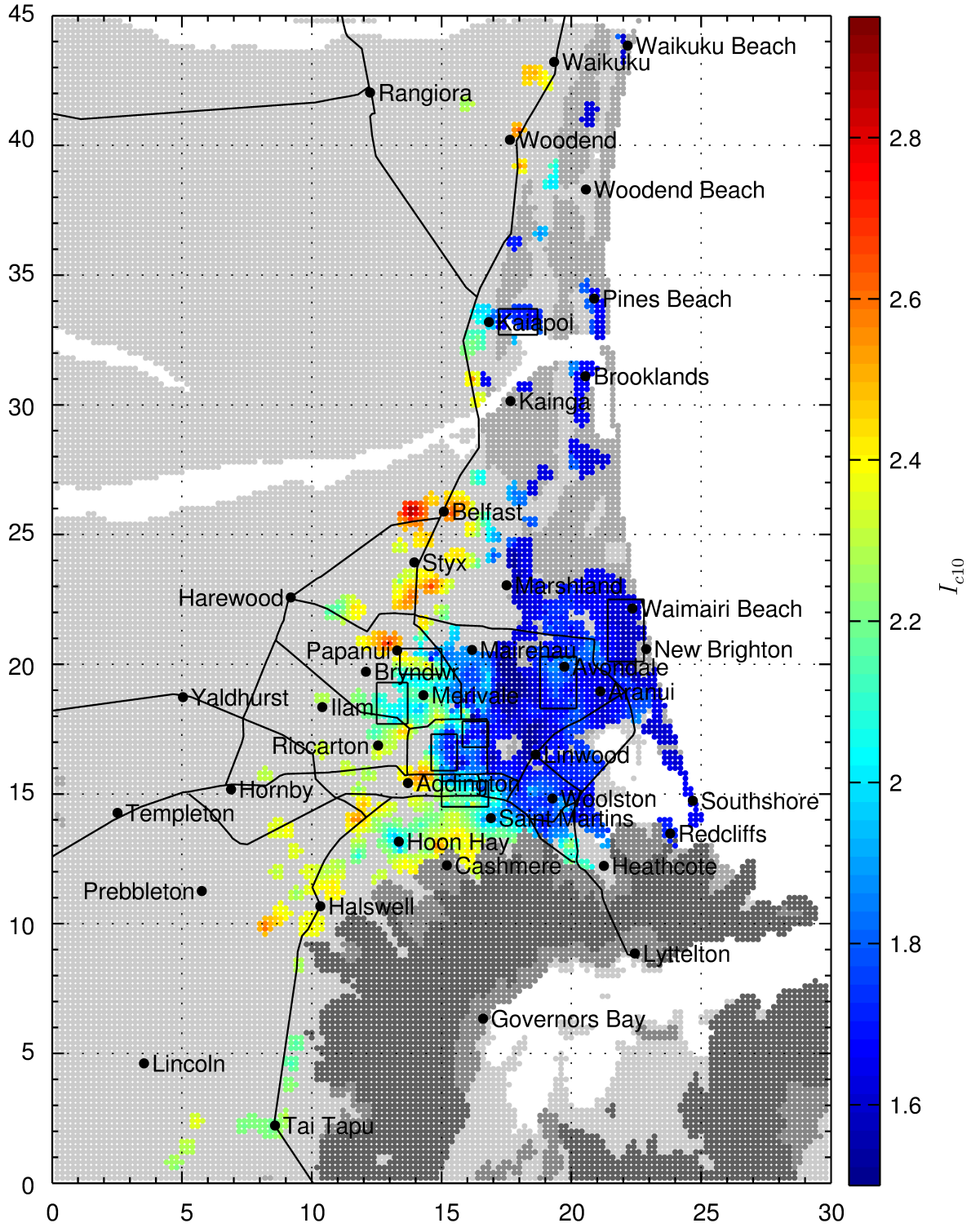

Fig. B.3: I_{c10} surface on uniform 200 × 200 m grid. NZMG projection; horizontal and vertical axes indicate km from lower left corner of map. Latitude/Longitude (WGS84) bounds for the map are (−43.6811°, 172.4418°) and (−43.2773°, 172.8151°). Predictions are only provided in each grid cell if there is one or more CPT record within 300 m.

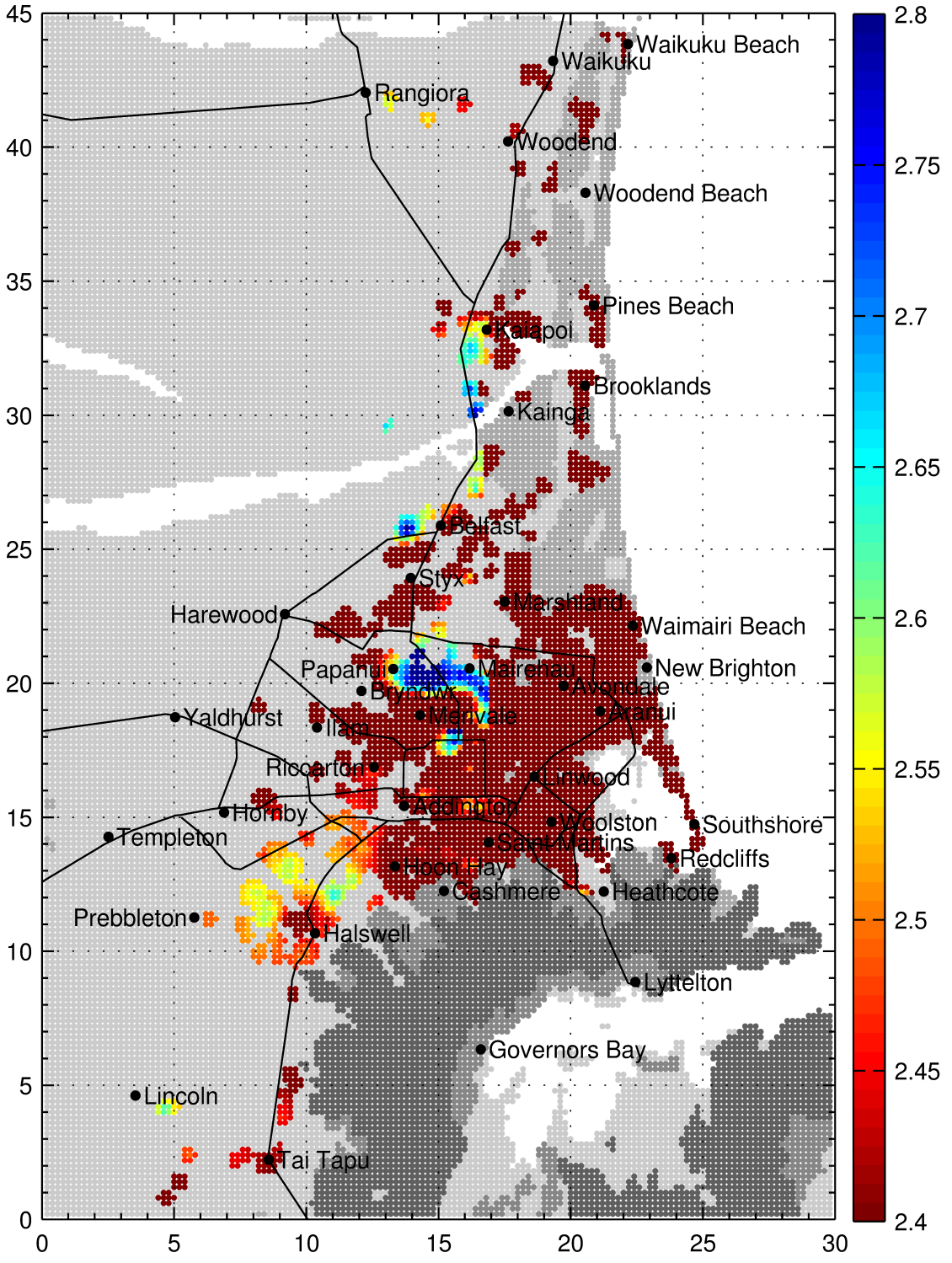

Fig. B.4: I_{c5} surface on uniform 200 × 200 m grid with narrow I_c scale. NZMG projection; horizontal and vertical axes indicate km from lower left corner of map. Latitude/Longitude (WGS84) bounds for the map are (−43.6811°, 172.4418°) and (−43.2773°, 172.8151°). Predictions are only provided in each grid cell if there is one or more CPT record within 300 m.

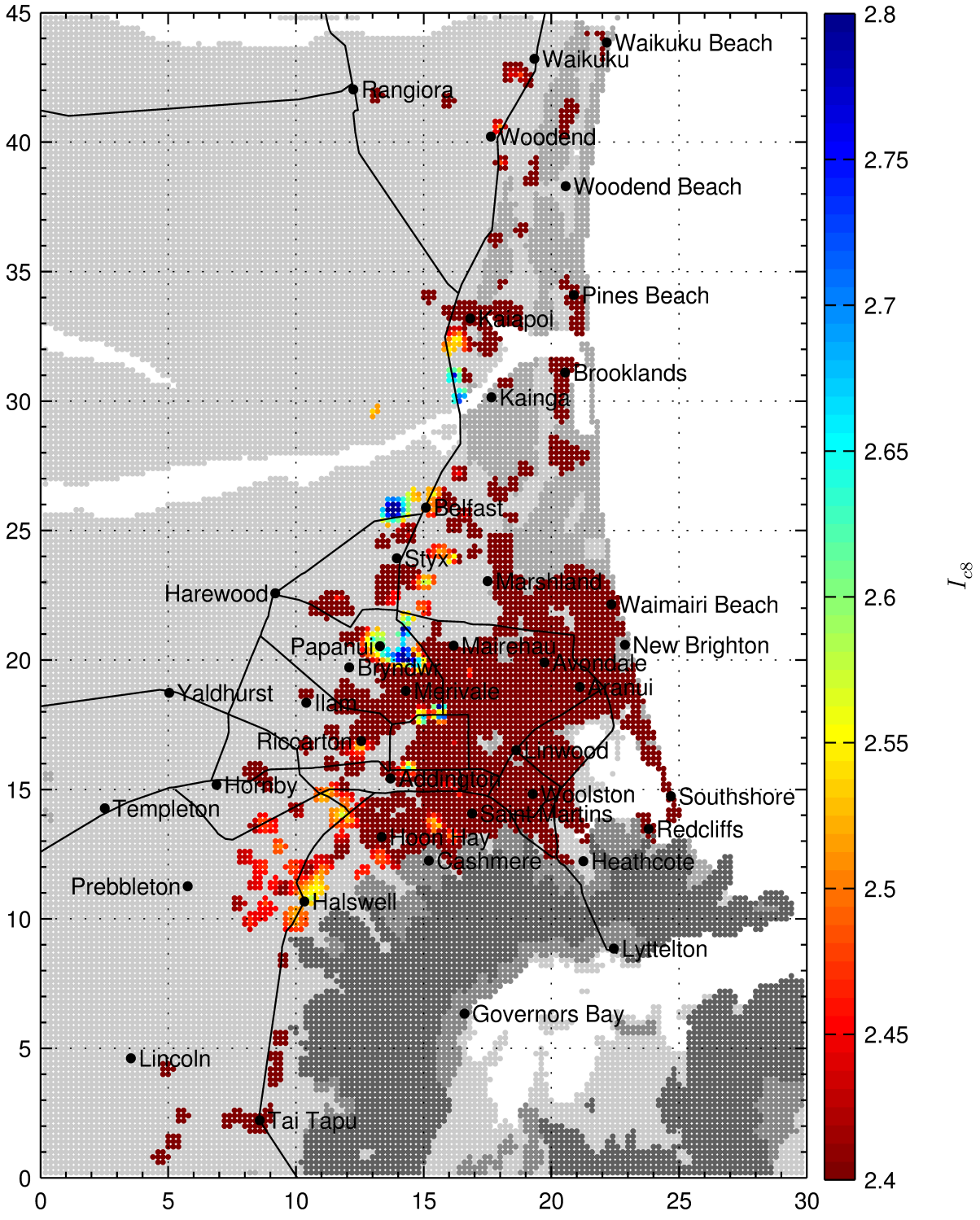

Fig. B.5: I_{c8} surface on uniform 200 × 200 m grid with narrow I_c scale. NZMG projection; horizontal and vertical axes indicate km from lower left corner of map. Latitude/Longitude (WGS84) bounds for the map are (−43.6811°, 172.4418°) and (−43.2773°, 172.8151°). Predictions are only provided in each grid cell if there is one or more CPT record within 300 m.

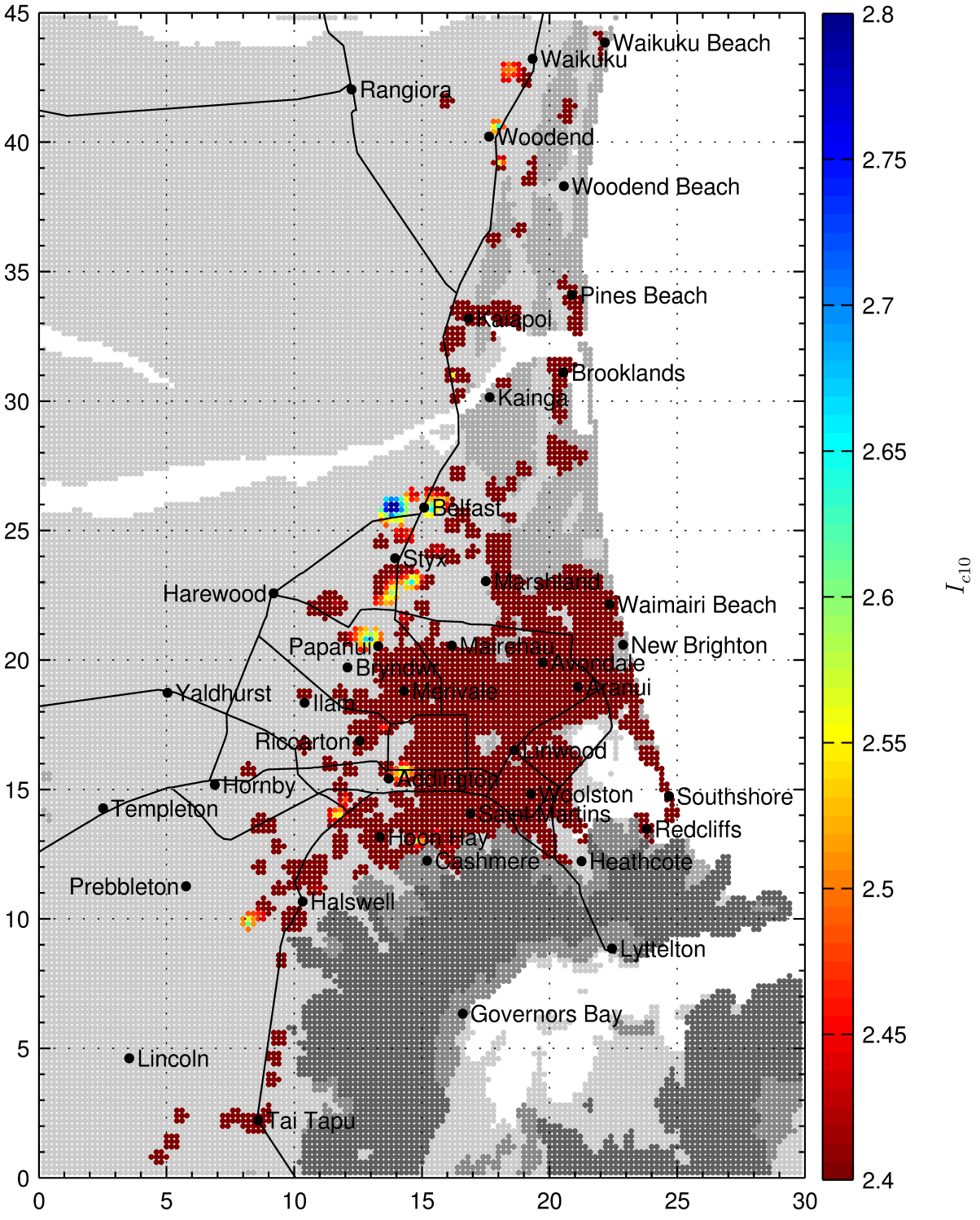

Fig. B.6: I_{c10} surface on uniform 200 × 200 m grid with narrow I_c scale. NZMG projection; horizontal and vertical axes indicate km from lower left corner of map. Latitude/Longitude (WGS84) bounds for the map are (−43.6811°, 172.4418°) and (−43.2773°, 172.8151°). Predictions are only provided in each grid cell if there is one or more CPT record within 300 m.